RESEARCH MEMORANDUM

ANALYSIS OF TURBOJET-ENGINE CONTROLS FOR AFTERBURNER STARTING

By W. E. Phillips, Jr.

Lewis Flight Propulsion Laboratory
Cleveland, Ohio

NATIONAL ADVISORY COMMITTEE
FOR AERONAUTICS

WASHINGTON

October 8, 1956

NACA RM E56F29

NATIONAL ADVISORY COMMITTEE FOR AERONAUTICS

RESEARCH MEMORANDUM

ANALYSIS OF TURBOJET-ENGINE CONTROLS FOR AFTERBURNER STARTING

By W. E. Phillips, Jr.

SUMMARY

A simulation procedure is developed for studying the effects of an afterburner start on a controlled turbojet engine. The afterburner start is represented by introducing a step decrease in the effective exhaust-nozzle area, after which the control returns the controlled engine variables to their initial values. The degree and speed with which the control acts are a measure of the effectiveness of the particular control system. Data are presented from an electronic analog computer study using the developed simulation procedure. For each of five systems investigated, it is possible to operate with turbine-discharge temperature overshoots of less than 3 percent of rated temperature, which eliminates the problem of damage to the turbine due to overtemperature in that region following an afterburner start. The steady-state errors of speed and temperature can also be reduced to negligible values in the two proportional control systems investigated.

Two major factors in the selection of a control are (1) initial speed undershoot, and (2) large engine fuel-flow overshoots and large initial decreases in effective exhaust-nozzle area when the afterburner is lit. These large deviations when associated with the initial speed undershoots are conducive to surge, particularly in engines with small surge margins. As the complexity of the control is increased by the addition of compensation, the severity of the speed, fuel-flow, and exhaust-nozzle-area transients is decreased, and the surge problem is correspondingly decreased. Complete compensation reduces the transient variations of all the variables to negligible amounts and therefore eliminates all surge problems during an afterburner start.

INTRODUCTION

A turbojet engine with an afterburner may be considered as having two basic modes of operation, nonafterburning and afterburning. The problems of control within the nonafterburning mode of operation have been investigated and reported previously and are not considered in this report. Within the afterburning mode of operation, steady-state operation

requires that the variable-area exhaust nozzle (necessary with afterburning) increase in area to maintain the basic engine variables at their rated values during afterburning. In the transition region between the two modes of operation, however, when the afterburner is lit or extinguished, accurate and fast control becomes a major problem. When the afterburner is lit at rated engine power, for example, initial transients of underspeed (resulting possibly in surge) and overtemperature (resulting possibly in turbine blade damage or surge) occur, which the control must quickly overcome. In general, the effects upon the engine variables of extinguishing the afterburner are the inverse of those associated with lighting the afterburner and are less dangerous. For this reason, only afterburner lighting is considered herein.

The object of this report is to investigate the effects of afterburner lighting on the engine behavior and control-system requirements of a controlled turbojet engine. The control systems considered are of the interacting type, discussed in theoretical terms in reference 1. An analog study of these interacting control systems for a turbojet engine operating only in the nonafterburning region is presented in reference 2. The basic control system considered herein is similar in configuration to that of reference 2. Engine rotor speed is controlled by engine fuel flow, and turbine-discharge temperature is controlled by the variable-area exhaust nozzle. The interaction referred to previously occurs within the engine, where the engine fuel flow has a considerable effect on the turbine-discharge temperature and the variable-area exhaust nozzle affects the engine rotor speed. Component additions to the control to minimize the interaction effects within the engine are considered in detail and are referred to as various forms of compensation.

In this report, a simulation procedure for the afterburner is developed (based on ref. 3), this afterburner simulation is coordinated with previously developed nonafterburning-engine simulation procedures (ref. 4), and the compensated interacting control systems of references 1 and 2 are used. The results of an analog investigation of the effects of an afterburner light on several controlled turbojet-engine configurations are reported and evaluated.

A closed-loop control rather than a nozzle-area-scheduling control is considered in this report because of the possibility that the afterburner will not ignite quickly on entry of the afterburner fuel flow. With the closed-loop control, the nozzle area will not change until the afterburner is lighted. Combustion delays in the afterburner were considered negligible. This is reasonable, because, although the delays are of the order of milliseconds, the afterburner combustion delays are not in the closed-loop portion of the control and thus will not affect the stability or steady-state characteristics of the system. Concerning transient response, the effect upon the engine of lighting the

afterburner is more severe if combustion delays are not considered. This report, then, presents the results for the most severe type of light - complete and immediate. The results may thus be tempered somewhat when applied to an actual engine.

3749

SYSTEM SIMULATION

The simulation technique for a controlled turbojet engine with afterburner is discussed in this section. The equations for the simulation of the engine are developed and discussed, a matrix representation of the engine and controllers is developed, and a block diagram for the systems dealt with is formulated.

CD-1 back

Nonafterburning Engine

The nonafterburning-engine equations are included in this discussion to serve as a basis for demonstrating the additional dynamics introduced by afterburning. For the nonafterburning engine, the input or independent variables are engine fuel flow and exhaust-nozzle area. The output or dependent variables usually chosen for control purposes are engine rotor speed and turbine-discharge temperature, and these dependent variables are used herein for both nonafterburning and afterburning studies.

The dynamic equations for the nonafterburning case are

$$\Delta N' = \left(\frac{K_{Nw_f}}{1 + \tau_e s}\right) \Delta w_f' + \left(\frac{K_{NA}}{1 + \tau_e s}\right) \Delta A' \tag{1}$$

$$\Delta T' = \left[K_{Tw_f} - K_{TN}K_{Nw_f}\left(\frac{\tau_e s}{1 + \tau_e s}\right)\right] \Delta w_f' + \left[K_{TA} - K_{TN}K_{NA}\left(\frac{\tau_e s}{1 + \tau_e s}\right)\right] \Delta A' \tag{2}$$

(Symbols are defined in appendix A, and nonafterburning equations are developed in appendix B. These equations are nondimensionalized. The primed engine variables represent percent changes based on the rated values, and the engine gain values are also normalized to the rated value of the variables; for example, $K_{Tw_f} = (\partial T/\partial w_f)_{A=\text{const}} \times w_{f,r}/T_r$.)

[redacted]

Equations (1) and (2) show that the engine speed response to either engine fuel flow or exhaust-nozzle area is a first-order lag, while the turbine-discharge temperature responses to these inputs are of a lead-lag form. With the exception of K_{TN}, the engine gains in equations (1) and (2) may be evaluated from steady-state data. The gain K_{TN} and the engine time constant τ_e must be evaluated from transient data.

Afterburning Engine

The dynamic equations for an afterburning engine are developed in appendix C, following the method of reference 4. The same engine variables are considered as in the nonafterburning case, with the addition of the independent variable w_b, the afterburner fuel flow. The response equations for engine rotor speed and turbine-discharge temperature are

$$\Delta N' = \left(\frac{K_{Nw_f}}{1 + \tau_e s}\right) \Delta w_f' + \left(\frac{K_{NA}}{1 + \tau_e s}\right) \Delta A' + \left(\frac{K_{Nw_b}}{1 + \tau_e s}\right) \Delta w_b' \tag{3}$$

$$\Delta T' = \left[K_{Tw_f} - K_{TN}K_{Nw_f}\left(\frac{\tau_e s}{1 + \tau_e s}\right)\right] \Delta w_f' + \left[K_{TA} - K_{TN}K_{NA}\left(\frac{\tau_e s}{1 + \tau_e s}\right)\right] \Delta A' + \left[K_{Tw_b} - K_{TN}K_{Nw_b}\left(\frac{\tau_e s}{1 + \tau_e s}\right)\right] \Delta w_b' \tag{4}$$

Comparison of equations (3) and (4) with equations (1) and (2) shows that afterburning introduces an additional term into each of the response equations.

As shown in appendix C, equations (3) and (4) may be reduced to

$$\Delta N' = \left(\frac{K_{Nw_f}}{1 + \tau_e s}\right) \Delta w_f' + \left(\frac{K_{NA}}{1 + \tau_e s}\right) \Delta A_{eff}' \tag{5}$$

$$\Delta T' \left[K_{Tw_f} - K_{TN}K_{Nw_f}\left(\frac{\tau_e s}{1 + \tau_e s}\right)\right] \Delta w_f' + \left[K_{TA} - K_{TN}K_{NA}\left(\frac{\tau_e s}{1 + \tau_e s}\right)\right] \Delta A_{eff}' \tag{6}$$

where $\Delta A_{eff}'$ represents an effective area

$$\Delta A_{eff}' = \Delta A' + \Delta A_{eq,b}' \tag{7}$$

The equations for afterburning are now analogous in form to those for nonafterburning, and previously developed nonafterburning simulation techniques may be used. It should be noted that the area considered in equations (5) and (6) is an effective area, composed of both the physical exhaust-nozzle area A and the variable $A_{eq,b}$. The variable $A_{eq,b}$ represents the equivalent resistance to flow of the tailpipe and the nozzle area due to afterburning. In steady-state afterburner operation, the effective area A_{eff} will be equal to the physical area A necessary to give rated engine speed and turbine-discharge temperature when not afterburning.

The magnitude of the $A_{eq,b}$ term must be evaluated to complete the afterburning-equation development. As developed from thermodynamic relations in appendix C, the thrust ratio (afterburning to nonafterburning) is

$$\frac{F_{j,b}}{F_{j,d}} = \frac{A_b}{A_d} \tag{8}$$

For the engine considered in this report, the maximum thrust ratio is 1.5, and A_d is 90 percent of rated area (rated area being the turbine-discharge area). Therefore,

$$A_b = 1.5\ A_d = 135 \text{ percent} \tag{9}$$

In this study, an exhaust-nozzle area $\Delta A'$ of 135 percent is taken to be the maximum physical opening of the exhaust nozzle, and the effect of afterburning is taken to be a 40-percent decrease in effective area ($\Delta A'_{eq,b} = -40$ percent). This establishes the steady-state values for nonafterburning and afterburning operation: for nonafterburning operation, $\Delta A' = 90$ percent, $\Delta A'_{eq,b} = 0$, and $\Delta A'_{eff} = 90$ percent; for afterburning operation, $\Delta A' = 130$ percent, $\Delta A'_{eq,b} = -40$ percent, and $\Delta A'_{eff} = 90$ percent. The 5-percent safety factor in $\Delta A'$ ensures that the turbine conditions will not exceed rated conditions in the steady-state afterburning condition.

The lighting of the afterburner is simulated by introducing a step in $\Delta A'_{eq,b}$ equivalent to a 40-percent decrease in exhaust-nozzle area. The block diagram of the system, including the engine, is given in figure 1.

Control Units and Sensor Units

The control units considered in this report are the engine fuel flow and the exhaust-nozzle-area control units. Each of these control

units is considered to consist of two parts, the dynamic terms of the basic servo power element and the gain and dynamic terms associated with the controller portions of the control unit. Thus, the control units consist of the relatively unchangeable servo power-element dynamics W_{w_f} and W_A and the flexible characteristics (the controller elements C_{w_fN} and C_{AT}) that may be varied to give the type of control desired.

The basic control units used in this report are included in figure 1. The terms C_{w_fN} and C_{AT} include the gain of the servo power element, the gain of the controller portion of the control unit, and the desired dynamics - that is, either proportional or proportional-plus-integral terms. For the studies to follow, in each particular system considered there are only two variable parameters, the gain of the fuel-flow controller C_{w_fN} (K_N) and the gain of the exhaust-nozzle-area controller C_{AT} (K_T). The controller matrix C has two additional elements, C_{w_fT} and C_{AN}, that have not been mentioned previously. These two elements are referred to as the compensation elements and are added to the control system to minimize (partial compensation) or eliminate (complete compensation) the interaction effects within the system. The use and results of the compensation terms are discussed in detail in the following sections.

The sensor units are those elements which convert the dependent variables (rotor speed and turbine-discharge temperature) into signals comparable with the reference inputs of the system. These are shown in figure 1. It is assumed for simplicity in this study that neither sensor unit (H_N and H_T) has any dynamics. This is a valid assumption, in that small pulse-type tachometers and high-response thermocouples are now being used in turbojet-engine control applications. The gain of the feedback elements, when nondimensionalized by normalizing to rated values, as was done with the engine gains, is unity. In the study presented in this report, then, both H_N and H_T are taken as unity at all frequencies.

Matrix Representation of Control System

A matrix representation of the complete controlled turbojet engine with afterburning has been developed, using the components and equations developed in the previous sections. The use of the matrix form simplifies any computations made for the system characteristics and also allows a more systematic approach to systems of the complexity considered in this report. The control units and sensor units are presented in an expanded matrix form in figure 1. The afterburning-engine equations may be put in a matrix form by introducing a frequency-independent (steady-state) matrix and a frequency-dependent (dynamic) matrix. This allows easier consideration of the steady-state operation of the control system.

A block diagram of the complete control system in matrix form is shown in figure 2. The elements of each matrix may be obtained from the expanded form shown in figure 1. In the following analysis, standard matrix subscripts are used in certain equations for clarity. The element S_{12}, for example, represents the element of the S matrix in the first row and second column and, from figure 1, corresponds to K_{NA}.

SYSTEM ANALYSIS

The analysis of a controlled turbojet engine with afterburning, of the form shown in figure 2, is discussed from an analytical point of view in this section. The analysis includes a development of the general system response equations, a discussion of the specific response equations associated with the uncompensated, partially compensated, and completely compensated systems for afterburner disturbances, and an example of the use of these equations through the calculation of the steady-state errors associated with the use of proportional or proportional-plus-integral control with each type of compensation. The complexity of the equations developed also illustrates the need for an analog solution of the transient responses of the systems considered.

The only system parameters that are varied in this study are the fuel-flow controller gain K_N and the exhaust-nozzle-area controller gain K_T. Since the data are a function primarily of loop gain rather than controller gain, the loop gains K_N^l and K_T^l are used throughout the data discussion, where

$$K_N^l = (\text{gain of loop from } \Delta N_e' \text{ to } \Delta w_f' \text{ to } \Delta N' \text{ to } \Delta N_e') = 0.45\ K_N$$

$$K_T^l = (\text{gain of loop from } \Delta T_e' \text{ to } \Delta A_{eff}' \text{ to } \Delta T' \text{ to } \Delta T_e') = 0.30\ K_T$$

Response Equations

The response equation, in matrix form, of the system shown in figure 2 is

$$c = (I + DSWCH)^{-1}(DSWC)r + (I + DSWCH)^{-1}(DS)d \tag{10}$$

or

$$c = \left(\frac{\text{adj } \Gamma}{|\Gamma|}\right)(DSWC)r + \left(\frac{\text{adj } \Gamma}{|\Gamma|}\right)(DS)d \tag{11}$$

where

$$\Gamma = I + DSWCH$$

The characteristic equation for the system is

$$|\Gamma| = |I + DSWCH| = 0 \tag{12}$$

Equation (11) may be broken up into three sets of equations, each of which deals with certain system properties.

The first set of equations defines the basic function of the control system, the response of each output variable to its corresponding reference input:

$$\Delta N' = \left[\left(\frac{\text{adj } \Gamma}{|\Gamma|}\right)(DSWC)\right]_{11} \Delta N_s' \tag{11a}$$

$$\Delta T' = \left[\left(\frac{\text{adj } \Gamma}{|\Gamma|}\right)(DSWC)\right]_{22} \Delta T_s' \tag{11b}$$

using standard matrix notation.

The second set of equations defines the interaction of the system, the response of each output to other than its corresponding reference input:

$$\Delta N' = \left[\left(\frac{\text{adj } \Gamma}{|\Gamma|}\right)(DSWC)\right]_{12} \Delta T_s' \tag{11c}$$

$$\Delta T' = \left[\left(\frac{\text{adj } \Gamma}{|\Gamma|}\right)(DSWC)\right]_{21} \Delta N_s' \tag{11d}$$

As developed previously, the afterburner effects may be considered equivalent to a change in effective area or, referring to figure 2, a load disturbance $\Delta A'_{eq,b}$. The response equations for this disturbance are

$$\Delta N' = \left[\left(\frac{\text{adj}\,\Gamma}{|\Gamma|}\right)(DS)\right]_{12} \Delta A'_{eq,b} \tag{11e}$$

$$\Delta T' = \left[\left(\frac{\text{adj } \Gamma}{|\Gamma|}\right)(DS)\right]_{22} \Delta A'_{eq,b} \qquad (11f)$$

The treatment of the system that is followed in this report is directly related to the six equations (11a) to (11f). It is desired to have each output variable follow its corresponding reference input as closely as possible (eqs. (11a) and (11b)), to minimize the response of the outputs to any but their corresponding inputs (eqs. (11c) and (11d)), and to minimize the effects of the afterburner operation upon the outputs (eqs. (11e) and (11f)).

Steady-State and Stability Calculations

Certain steady-state and stability properties of the systems investigated may be determined analytically. These calculated values provide basic knowledge of the systems and also establish checking data to verify the analog solution.

The stability of an interacting system is a function of both K_N^l and K_T^l. The stability of a given system may be plotted as a stability contour with K_N^l and K_T^l as coordinates, and this method is used with analog data. The stability equation (12) is too complex to attempt to obtain a complete contour analytically. However, the end points of the stability contour (K_N^l with $K_T^l = 0$ and K_T^l with $K_N^l = 0$) may be calculated, and this gives an approximate value of the range of gains encountered within the stable region of operation.

The output final values may be calculated from the steady-state coefficiert matrix equations:

$$\lim_{t\to\infty} c(t) = \lim_{s\to 0}\left\{s\left[\left(\frac{\text{adj } \Gamma}{|\Gamma|}\right) DSWC\right] r(s)\right\} = \varphi[r(t)]_{t=\infty} \qquad (13a)$$

$$\lim_{t\to\infty} c(t) = \lim_{s\to 0}\left\{s\left[\left(\frac{\text{adj } \Gamma}{|\Gamma|}\right) DS\right] d(s)\right\} = \theta[d(t)]_{t=\infty} \qquad (13b)$$

The approximate range of gains determined by the stability-contour end points may be used to evaluate the general range of steady-state values for each system.

The actual values of the system matrices shown in figure 2 (assuming engine operation at rated dry thrust) are

Engine matrices:

$$D = \begin{bmatrix} \frac{1}{1 + 1.75\ s} & 0 \\ \frac{0.70\ s}{1 + 1.75\ s} & 1 \end{bmatrix} \qquad S = \begin{bmatrix} 0.45 & 0.67 \\ 0.40 & -0.30 \end{bmatrix}$$

Controller matrix:

C elements (form and values are covered in later discussions)

Servo matrix:

$$W = \begin{bmatrix} \frac{1}{(1 + 0.1\ s)^2} & 0 \\ 0 & \frac{1}{(1 + 0.2\ s)(1 + 0.4\ s)} \end{bmatrix}$$

From these values and the various equations presented in this section, the stability-contour end points are determined and the final values of equations (11a) to (11f) evaluated and tabulated. The values of the θ matrix (eq. (13b)) are calculated for a step input of unity [$\Delta A'_{eq,b}(t) = U(t)$]. The coefficient θ_{12} relates engine speed to $\Delta A'_{eq,b}$, and the coefficient θ_{22} relates turbine-discharge temperature to $\Delta A'_{eq,b}$. Controllers (C matrix) of both proportional and proportional-plus-integral form are considered in this analytic discussion.

Uncompensated system. - The basic interacting system, with $C_{wfT} = C_{AN} = 0$, is termed the uncompensated system. The interaction in this system occurs through the engine matrices D^{-} and S, because the remainder of the system matrices are diagonals.

For the proportional control of the uncompensated system, the C matrix is

$$C = \begin{bmatrix} K_N & 0 \\ 0 & -K_T \end{bmatrix} \tag{14a}$$

and, for the proportional-plus-integral control, the C matrix is

$$C = \begin{bmatrix} K_N\left(1 + \frac{1}{1.75\ s}\right) & 0 \\ 0 & -K_T\left(1 + \frac{1}{1.75\ s}\right) \end{bmatrix} \tag{14b}$$

The temperature-to-area controller gain $-K_T$ must be negative for stability, because the engine gain K_{TA} is negative. The integral time constants (1.75 sec) are chosen equal to the engine time constant τ_e.

The values of the stability-contour end points for both the proportional and proportional-plus-integral uncompensated systems were calculated from equation (12) and are presented in table I. Table I shows that the stability-contour end points for both uncompensated systems investigated are finite, which means that care must be taken in adjusting the gains to obtain a stable system.

The steady-state coefficients θ_{12} and θ_{22} (eq. (13b)) were calculated for step inputs of unit amplitude [$\Delta A'_{eq,b}(t) = U(t)$] and are presented in table II. This tabulation shows that in the uncompensated proportional system each output ($\Delta N'$ and $\Delta T'$) will have a steady-state error associated with the afterburner disturbance $\Delta A'_{eq,b}$. These errors are functions of both the speed loop gain K_N^l and the temperature loop gain K_T^l. The uncompensated proportional-plus-integral system, as might be expected, will have no steady-state errors. The outputs ($\Delta N'$ and $\Delta T'$) in steady state will be unaffected by the afterburner disturbance ($\theta_{12} = \theta_{22} = 0$).

Therefore, the addition of integral control to the uncompensated system, in eliminating steady-state errors, eliminates the steady-state interaction effects. However, the interaction still exists in the transient case for both the proportional and proportional-plus-integral controls.

Completely compensated system. - The term "completely compensated system" applies to the system wherein the controller elements $C_{w_f T}$ and C_{AN} are so chosen that $\Delta N'$ is unaffected by $\Delta T'_s$ and $\Delta T'$ is is unaffected by $\Delta N'_s$, for both steady-state and transient considerations. Referring to equations (11c) and (11d) for complete compensation, it follows that

$$\left[(\Gamma)^{-1}_{DSWC}\right]_{12} = \left[(\Gamma)^{-1}_{DSWC}\right]_{21} = 0 \tag{15a}$$

[redacted]

Equation (15a) will be satisfied if

$$(DSWC)_{12} = (DSWC)_{21} = 0 \tag{15b}$$

since equation (15b) will make $(\Gamma)^{-1}$ a diagonal matrix. Solving equation (15b) for the elements C_{w_fT}/C_{AT} and C_{AN}/C_{w_fN} yields

$$\frac{C_{w_fT}}{C_{AT}} = -\frac{(D_{NN}S_{NA} + D_{NT}S_{TA})W_A}{(D_{NN}S_{Nw_f} + D_{NT}S_{Tw_f})W_{w_f}} \tag{16a}$$

$$\frac{C_{AN}}{C_{w_fN}} = -\frac{(D_{TT}S_{Tw_f} + D_{TN}S_{Nw_f})W_{w_f}}{(D_{TT}S_{TA} + D_{TN}S_{NA})W_A} \tag{16b}$$

The controller matrix elements thus are similar to those of equations (14a) and (14b), with the addition of the proper values of C_{w_fT} and C_{AN} from equations (16a) and (16b).

The elements C_{w_fT} and C_{AN} by definition eliminate both the steady-state and transient interaction effects encountered in the uncompensated system. This means that the system is uncoupled and two independent loops now exist. This uncoupling is demonstrated by considering the stability equation (12). Consideration of equation (15a) and the fact that the H matrix is an identity matrix yields for the stability equation

$$|\Gamma| = |I + DSWCH| = [1 + (DSWC)_{11}]\ [1 + (DSWC)_{22}] = 0 \tag{17a}$$

which in turn gives

$$1 + (DSWC)_{11} = 0 \tag{17b}$$

$$1 + (DSWC)_{22} = 0 \tag{17c}$$

as the two independent characteristic equations for the completely compensated system. The stability contour for this system will consist of two straight lines, one independent of K_N^l (eq. (17c)) and one independent of K_T^l (eq. (17b)). The values shown in table I indicate that, with either proportional or proportional-plus-integral control, the completely compensated system is stable for all positive values of loop gains.

[redacted]

Considering table II, with the completely compensated proportional system, the uncoupling of the system is indicated by the fact that the steady-state coefficients θ_{12} and θ_{22} are functions only of their respective loop gains. The area disturbance $\Delta A'_{eq,b}$ introduces a disturbance directly into the temperature loop and into the speed loop through the engine term $(DS)_{12}$. Once this $\Delta A'_{eq,b}$ disturbance is introduced into each loop, the loops are uncoupled. The use of the proportional-plus-integral control with the completely compensated system eliminates the steady-state errors associated with the proportional control.

The uncoupling of the system may also be illustrated by consideration of the response equations (11e) and (11f). Realizing that for this system

$$(DSWC)_{12} = (DSWC)_{21} = 0 \tag{15b}$$

the response equations become

$$\Delta N' = \left[\frac{(DS)_{12}}{1 + (DSWC)_{11}}\right]\Delta A'_{eq,b} \tag{18a}$$

$$\Delta T' = \left[\frac{(DS)_{22}}{1 + (DSWC)_{22}}\right]\Delta A'_{eq,b} \tag{18b}$$

These equations illustrate the steady-state and transient uncoupling of the interacting system and complete the analysis of the completely compensated system for afterburner lights.

Partially compensated system. - The partially compensated system is a compromise between the uncompensated and completely compensated systems. The elements C_{w_fT} and C_{AN} are simplified from those of the completely compensated system to the extent that the system is uncoupled only for steady-state operation. However, reference 2 found that partial compensation also improves the transient capabilities of the system, and it is primarily for this reason that partial compensation is considered. The terms C_{w_fT}/C_{AT} and C_{AN}/C_{w_fN}, as an extension of equations (16a) and (16b), are

$$\frac{C_{w_fT}}{C_{AT}} = -\left[\frac{(D_{NN}S_{NA} + D_{NT}S_{TA})W_A}{(D_{NN}S_{Nw_f} + D_{NT}S_{Tw_f})W_{w_f}}\right]_{s=0} \tag{19a}$$

$$\frac{C_{AN}}{C_{w_fN}} = -\left[\frac{(D_{TT}S_{Tw_f} + D_{TN}S_{Nw_f})W_{w_f}}{(D_{TT}S_{TA} + D_{TN}S_{NA})W_A}\right]_{s=0} \tag{19b}$$

The controller matrices again are similar to those of equations (14a) and (14b), with the addition of C_{w_fT} and C_{AN} from equations (19a) and (19b).

Since the system is uncoupled only for steady-state operation, the stability equation for the partially compensated system will not reduce to two independent equations as it did for the completely compensated system. The stability-contour end points were calculated and are shown in table I. The temperature loop considered alone is inherently stable ($K_T^l = \infty$ for instability), while the speed loop instability gain has a finite value.

The uncoupling of the partially compensated system in steady-state operation is illustrated in table II by the steady-state coefficients θ_{12} and θ_{22} for the proportional control. As in the completely compensated proportional case; the coefficients are functions only of their respective loop gains. The use of the proportional-plus-integral control with the partially compensated system eliminates the steady-state errors associated with the proportional control. The effect of partial compensation can only be determined from analog data, as even approximations in an analytical transient study would become too complex.

Summary of Analytical Results

The analytical results serve mainly as a guide to the more complete analog study that follows. The addition of complete compensation to the basic uncompensated system uncoupled the system in both steady-state and transient operation, while the addition of partial compensation uncoupled the system only in steady-state operation. Since partial compensation is considerably less complex to add to the system, it is hoped that partial compensation will improve the transient response compared with the uncompensated system sufficiently to warrant its use in cases where the requirements do not necessitate use of the more complex complete compensation.

The analog computer study, as discussed previously, is necessary to evaluate the complete stability contour and the transient behavior of the systems considered. All the systems included in table II, except the uncompensated proportional system, are included in the analog computer study.

ANALOG SIMULATION

The computer used for the analog analysis of the effects of an afterburner light on a controlled turbojet engine was an electronic differential analyzer, operating with a real time base. The variables recorded on a direct-writing oscillograph were engine speed $\Delta N'$, turbine-discharge temperature $\Delta T'$, afterburner disturbance $\Delta A'_{eq,b}$, exhaust-nozzle area $\Delta A'$, and engine fuel flow $\Delta w_f'$.

Five of the systems investigated analytically in the previous section were investigated on the analog computer:

(1) Uncompensated proportional-plus-integral

(2) Partially compensated proportional

(3) Partially compensated proportional-plus-integral

(4) Completely compensated proportional

(5) Completely compensated proportional-plus-integral

These systems were set up on the analog with techniques discussed in references 2 and 4 and following the block diagram of figure 2. As mentioned previously, the only system parameters considered variable in this study are the controller gains K_N and K_T, and these were simulated by variable coefficient units.

The physical area $\Delta A'$ has limits of travel on the actual engine, and these were simulated by limiting the variable $\Delta A'$ in the analog setup. The lower limit was set at $\Delta A' = 75$ percent, and the upper limit at $\Delta A' = 135$ percent. The physical exhaust-nozzle area at rated engine speed and turbine-discharge temperature is 90 percent.

The stability-contour end points and the steady-state errors determined analytically were used to check each system setup before the data were taken.

RESULTS AND DISCUSSION

In a single-loop system, if the transient response to a step in load disturbance is considered as a function of the loop gain, an increase in gain typically results in a faster response and a decrease in overshoot and steady-state error, until the system reaches the limit of stable operation. The same general dependence on the loop gain is observed in a controlled interacting system of the type discussed in this report, but in this case both loop gains affect the transient response and the stability limit of the system.

The information necessary to define the operation of a controlled interacting system includes definition of the stable region of operation and determination of the steady-state errors and the transient responses within the stable operating region. In obtaining the analog data, the boundary of the stable region of operation (the stability contour) was determined as a function of the loop gains, and the steady-state errors and transient responses to the afterburner light [$\Delta A'_{eq,b} = -40\ U(t)$] were recorded for sets of loop gains within the stable region. It is possible, then, with the analog data taken, to determine the following for given loop gains K_N^l and K_T^l: whether the system is stable; if stable, the transient and steady-state responses to the afterburner light; if the responses are not acceptable, what variations if K_N^l and K_T^l will improve the response; and if either partial or complete compensation of the control system will improve the system response.

Performance Criteria

It is necessary to establish performance criteria for comparing the operation of the five systems investigated. The criteria also allow a concise representation of the performance of each system, as these criteria may be plotted as functions of the loop gains. Examples of the analog traces obtained are shown in figure 3. The performance criteria chosen are labeled on these curves. The transient criteria considered are the engine speed undershoot and the turbine-discharge temperature overshoot; and, for the systems without integral control, the steady-state errors are also considered.

Three types of plots were useful in defining the system behavior. One type is contour lines of constant values of the transient performance criteria with K_N^l the ordinate and K_T^l the abscissa. The stability contour for the particular system considered is also included in this type of plot (e.g., fig. 4(a)). The plot is useful in determining rapidly the relation of a given operating point to the stability contour and the performance criteria at the operating point, but it is difficult to determine the permissible performance criteria for the system.

In order to determine the permissible performance criteria for each system and to facilitate comparison between the various types of systems considered, a second type of plot is used. In this plot, the permissible combinations of the transient performance are used as the coordinates and yield a bounded region as shown in figure 4(b). Owing to instability, it is impossible to obtain the performance criteria in the cross-hatched portion of figure 4(b), and the line thus represents the limit of performance obtainable. This plot indicates immediately

the permissible performance criteria obtainable and provides a good method of comparing systems. The third type of plot is used where the criteria depend on only one loop gain. Figure 6(c) is an example of this type of plot.

A measure of the speed of response would also be desirable in evaluating the transient response properties of the various systems investigated. No suitable criteria were found for this, however; therefore, for each system, sample traces are included to show not only speed of response, but other characteristics as well.

System Data Discussion

Uncompensated proportional-plus-integral system. - The performance criteria and the stability contour for the uncompensated proportional-plus-integral system are plotted as functions of the loop gains in figure 4(a). The interaction of this system is apparent in the diagonal nature of these characteristics. A general trend is observed of decreasing engine speed undershoot with an increase in either K_N^l or K_T^l, while a decreasing turbine-discharge temperature overshoot occurs with an increase in K_T^l or a decrease in K_N^l. Of the six operating points shown in figure 4(a) (1𝒰 to 6𝒰), point 6𝒰 appears to be the best; and this is borne out in the permissible performance criteria plot of figure 4(b). A comparison of figures 4(a) and (b) shows that the boundary of the permissible region of operation in figure 4(b) corresponds to a portion of the stability contour in figure 4(a). While point 6𝒰 represents the only data taken in the low temperature overshoot region, it appears that a further decrease in K_N^l and a corresponding increase in K_T^l will provide a lower temperature overshoot (< 6 percent). The most important point to be gained from figure 4(b), however, is the fact that, for the uncompensated proportional-plus-integral system investigated, it is impossible to operate with an engine speed undershoot of less than 6 percent for temperature overshoots under 10 percent.

The analog traces for the six points (1𝒰 to 6𝒰) shown in figures 4 are presented in figure 5. The sensitivities of each variable and the positive or increasing direction are included on the traces. The traces show that the response at point 6𝒰 is considerably underdamped; and, for this reason, a compromise between points 5𝒰 and 6𝒰 would be more desirable, despite the fact that the performance criteria are higher at point 5𝒰. Examination of the six sets of traces shows that the response time is a function of the combination of K_N^l and K_T^l and increases with a decrease in either K_N^l or K_T^l. Thus, the response times of points 5𝒰 and 6𝒰, with low values of K_N^l, are somewhat longer than those

of the points with higher K_N^1 but are still acceptable, since the transients are essentially finished within 5 seconds.

The limiting action as the exhaust nozzle reaches its maximum opening is clearly seen in the $\Delta A'$ traces, and this limiting action causes the nonlinear character of the other response traces. The overshoots in engine fuel flow vary from 60 percent at point 1% to 8 percent at point 6%. While the assumption of linearity of the engine parameters would not hold for $\Delta w_f'$ overshoots of 60 percent, operation at this point would not be recommended because of high $\Delta T'$ overshoots incurred, and it is felt that the trends indicated in the region of point 1% will hold. For $\Delta w_f'$ overshoots not in excess of 20 percent, the linearity of the engine is assumed to be correct, and therefore any data points are assumed correct.

The optimum region of operation for the uncompensated proportional-plus-integral control system has been determined to be in the region of points 5% and 6%, with a $\Delta T'$ overshoot of approximately 8 percent and a $\Delta N'$ undershoot, limited by the characteristics of the system, of over 6 percent. The transient response is slightly underdamped and essentially is over in 5 seconds. These performance criteria, while within acceptable limits, are dangerous in engines with a small margin between the steady-state operating line and the surge line. The $\Delta N'$ undershoot, $\Delta w_f'$ overshoot, and initial $\Delta A_{eff}'$ decrease all tend to drive the engine into the surge region. For this reason, the uncompensated proportional-plus-integral system investigated is not recommended for afterburner operation, unless the turbojet engine has a large surge margin, which may be determined from consideration of the engine characteristics and the optimum performance criteria.

Partially compensated proportional system. - The performance criteria and the stability contour for the partially compensated proportional system are plotted as functions of the loop gains in figure 6(a). The interaction of the system is again apparent in the diagonal nature of these characteristics. Of the six operating points shown in figure 6(a), point 6% yields the smallest performance criteria values, and this is borne out in the permissible performance criteria plot of figure 6(b). The plot of figure 6(b) shows, similar to the uncompensated system, that it is impossible to operate with less than 5-percent speed undershoot for reasonable values of temperature overshoot.

The curves of the speed and temperature steady-state errors are plotted as functions of the loop gains in figures 6(c) and (d), respectively. Each steady-state error depends only on its respective loop gain. This agrees with the formulas in table II for the partially compensated proportional system, and good agreement is obtained between the analog and analytical data (figs. 6(c) and (d)). As expected, an

increase in either loop gain decreases the associated steady-state error. Operation at point 6$\mathscr{P}$ gives a reasonable value for steady-state speed error and negligible steady-state temperature error.

The analog traces for the six points 1$\mathscr{P}$ to 6$\mathscr{P}$ shown in figures 6 are presented in figure 7. As in the uncompensated system, the analog traces show that point 6$\mathscr{P}$ is considerably underdamped, and a compromise with the more stable characteristics of point 5$\mathscr{P}$ is desirable. Examination of the traces shows that the response time is a function only of the speed loop gain and increases with a decrease in K_N^l. Operation in the region of points 5$\mathscr{P}$ and 6$\mathscr{P}$ provides good time of response, with the transient essentially over in 2 seconds.

Therefore, the optimum region of operation for the partially compensated proportional system is in the region of points 5$\mathscr{P}$ and 6$\mathscr{P}$, with a negligible $\Delta T'$ overshoot and a $\Delta N'$ undershoot, limited by the characteristics of the system, of over 5 percent. The transient response is slightly underdamped, and the transient is essentially over in 2 seconds. Because of the negligible temperature overshoot in this system, the surge problem would be much less of a consideration than with the uncompensated proportional-plus-integral system. The main disadvantage of the partially compensated proportional system is the steady-state speed error. A discussion of the addition of the integral terms to eliminate the steady-state speed error follows.

Partially compensated proportional-plus-integral system. - The performance criteria and the stability contour for the partially compensated proportional-plus-integral system are plotted as functions of the loop gains in figure 8(a). Comparison of this plot with figure 6(a) shows that the addition of the integral term did not materially effect either the stability contour or the performance criteria. The integral term did, however, eliminate the steady-state errors associated with the partially compensated proportional system. Of the six operating points shown in figure 8(a), point 12$\mathscr{P}$ appears to be the best, and this is verified by the permissible performance criteria plot of figure 8(b). As with the proportional system, it is impossible to operate with less than 5-percent speed undershoot for reasonable values of temperature overshoot.

The analog traces for the six points 7$\mathscr{P}$ to 12$\mathscr{P}$ shown in figures 8 are presented in figure 9. As in the proportional system, the analog traces show that the responses at point 12$\mathscr{P}$ are considerably underdamped, and again a compromise with a point of more stable operation is desirable. The traces show that the response time is primarily a function of the speed loop gain, as in the proportional system. Operation in the region of points 11$\mathscr{P}$ and 12$\mathscr{P}$ provides a response time of about 3 seconds, somewhat longer than the proportional system, but still acceptable. The interesting fact to notice with this system is the

type of $\Delta w_f'$ transient obtained. In traces 9$\mathscr{P}$, 11$\mathscr{P}$, and 12$\mathscr{P}$, the $\Delta w_f'$ initially undershoots, as contrasted with the high $\Delta w_f'$ overshoots encountered in the uncompensated proportional-plus-integral system (fig. 5). The $\Delta w_f'$ signal in the partially compensated system is a sum of two signals, one of which is $\Delta N_e'$ through the element $C_{w_f N}$ and the other is $\Delta T_e'$ through the element $C_{w_f T}$. Since $C_{w_f T}$ has a negative modulus, the portion of the $\Delta w_f'$ signal through $C_{w_f T}$ produces the $\Delta w_f'$ undershoot.

The $\Delta w_f'$ undershoot of 2 percent at point 12$\mathscr{P}$ considerably diminishes the surge problem for this system; and, with the exception of the 5-percent $\Delta N'$ undershoot, the partially compensated proportional-plus-integral system provides very good performance criteria.

Completely compensated proportional system. - As discussed previously in the analysis of the completely compensated system, the interaction is eliminated by the addition of the crossover terms specified by equations (16a) and (16b). This means that there are now two independent loops; and, referring to equations (18a) and (18b), the speed response is a function only of the speed loop gain K_N^l, and the temperature response is a function only of the temperature loop gain K_T^l.

The stability contour and permissible performance criteria plots thus have little significance with the completely compensated systems. The plots of speed and temperature steady-state errors presented in figures 10(a) and (b), respectively, show that, as either loop gain is increased, the corresponding steady-state error is decreased. Operation of the system at the K_N^l value corresponding to point 6$\mathscr{C}$ and the K_T^l value corresponding to point 3$\mathscr{C}$ yields very acceptable steady-state errors of less than 0.5 percent. Both loops are inherently stable, as shown by the values of infinity in table I.

The analog traces for the six points 1$\mathscr{C}$ to 6$\mathscr{C}$ shown in figures 10 are presented in figure 11. These analog traces illustrate several interesting facts about this system. Considering first the form of the responses, there is an initial high-frequency transient which is a function of the loop gains and a slower final transient rising to the final value. The size of the initial transients increases as the loop gain is increased, and slight overshoot of the temperature occurs at high K_T^l values (point 3$\mathscr{C}$). The response time is not too important a criterion for this system because of the almost negligible steady-state errors encountered at high loop gain.

The $\Delta w_f'$ transient may be approximated by summing the responses at points 3¢ and 6¢. The resultant trace yields a short-duration overshoot of approximately 2 percent and a positive steady-state $\Delta w_f'$ error of 1 percent. The exhaust-nozzle area responds within 0.1 second, as shown on the traces of figure 11. This means that the transient deviations of $\Delta A_{eff}'$ are very small and of very short duration. These small values, coupled with the negligible $\Delta N'$ and $\Delta T'$ deviations, mean that surge would not be encountered with this control, even in engines with a small surge margin.

3749

Completely compensated proportional-plus-integral system. - As with the proportional system, the interaction is eliminated in the completely compensated proportional-plus-integral system, and the stability contour and permissible performance criteria plots have little significance.

The curves of engine speed undershoot and temperature overshoot as functions of their respective loop gains are given in figures 12(a) and (b), respectively. These performance criteria decrease as the loop gains are increased. Operation of the system at the K_N^l value corresponding to point 12¢ and the K_T^l value corresponding to point 9¢ yields transient deviations of less than 0.25 percent. The steady-state errors are eliminated by the integral term.

The analog traces for the six points 7¢ to 12¢ shown in figures 12 are presented in figure 13. The initial form of the transient is very similar to the high-frequency portion of the traces observed in the proportional system. The final portions of the transients are similar in response time, although in this system the steady-state error goes to zero because of the integral control. As with the proportional systems, because of the small transient deviations possible (points 9¢ and 12¢), the response time is not a significant performance criterion.

The summing of the $\Delta w_f'$ traces of points 9¢ and 12¢ again reveals a slight initial overshoot, which for this system is approximately 1.5 percent. This small value, combined with the negligible $\Delta N'$, $\Delta T'$, and $\Delta A_{eff}'$ transient deviations, again means that the surge problem is nonexistent with this system if operation is maintained with high loop gains.

Comparison of systems investigated. - The permissible performance criteria plots of the uncompensated and partially compensated systems are compared in figure 14. As discussed previously, there are no permissible performance criteria plots for the completely compensated systems, but a region of reasonable operating gains may be included,

as shown by the shaded region in figure 14. The comparisons presented in this section are based on the performance criteria obtained at the best operating regions for each system, as determined in the preceding discussions. Referring to figure 14, the improvement obtained with the addition of partial compensation is evidenced mainly in the reduction from 6 percent to 5 percent of the value of the minimum speed undershoot obtainable for reasonable values of temperature overshoot. The complete compensation reduced the speed undershoot and the temperature overshoot to negligible values by uncoupling the two loops and thus making these performance criteria independent of each other.

In the proportional systems it was possible to operate at points giving small steady-state errors, and the integral controls eliminated these steady-state errors entirely. The time the transients took to reduce essentially to zero was less than 5 seconds for the optimum operating regions in all five systems, which is well within acceptable limits for control operation.

The major problems with the control configuration of $\Delta w_f'$ to $\Delta N'$ and $\Delta A'$ to $\Delta T'$ during an afterburner light are excessive overshoot of $\Delta T'$ and the possibility of surge due to a combination of high $\Delta w_f'$ overshoots, $\Delta N'$ undershoots, and a large initial decrease in $\Delta A_{eff}'$ until the exhaust nozzle opens to compensate for the afterburner light. The data show that, for each system, the $\Delta T'$ overshoot may be reduced below 1 percent, and overtemperature damage is thus eliminated as a problem for consideration. The surge problem, however, exists in both the uncompensated and partially compensated systems. Engine surge is particularly likely to occur in the uncompensated system because of initial undershoot in $\Delta N'$, an overshoot in $\Delta w_f'$, and a decrease in $\Delta A_{eff}'$. In the partially compensated systems, the crossover terms $C_{w_f T}$ and C_{AN} introduce signals that cause the $\Delta w_f'$ to initially undershoot, which considerably diminishes the possibility of surge. The effective area response is somewhat faster for the partially compensated systems, and the speed undershoot is smaller, decreasing further the possibility of surge in this system. The major improvements exhibited by the addition of complete compensation to the basic control system are the reduction to negligible values of the $\Delta N'$ undershoot and the very fast response of the exhaust-nozzle area $\Delta A'$, effectively eliminating the large initial decrease in the effective area $\Delta A_{eff}'$. Small $\Delta w_f'$ overshoots are obtained with the completely compensated system but are of too small an order to cause surge. Therefore, complete compensation entirely eliminates any possibility of surge with the form of control considered.

SUMMARY OF RESULTS

A simulation procedure was developed for studying the effects of an afterburner light upon a controlled turbojet engine. The afterburner light may be represented by introducing a step decrease in the exhaust-nozzle area, after which the control will act to return the controlled engine variables to their values before the afterburner was lit. The degree and speed with which the control returns these variables to their initial values are a measure of the effectiveness of the particular control system being studied.

For each of the five systems investigated, it is possible to operate with turbine-discharge temperature overshoots of less than 3 percent, which eliminates the problem of damage to the turbine caused by overtemperature in the turbine region following an afterburner light. It is also possible to reduce the steady-state errors of speed and temperature in the two proportional controller systems investigated to negligible values.

The initial speed undershoot is one of two major factors in the selection of the type of control to use. The uncompensated and partially compensated systems have limiting values of speed undershoot of 6 percent and 5 percent, respectively, below which it is impossible to operate without instability. With complete compensation it is possible to operate with speed undershoots well below 1 percent.

The other major factors in the type of control to use are the large engine fuel-flow overshoots and the large initial decreases in the effective exhaust-nozzle area when the afterburner is lit. These large deviations when associated with initial undershoots in engine speed are very conducive to surge, particularly in engines with a small margin between the steady-state operating line and the surge line. For the uncompensated system operating in the optimum gain region, fuel-flow overshoots of 8 percent and initial effective exhaust-nozzle-area decreases of 40 percent for an interval of approximately 0.5 second were obtained. For the partially compensated systems, the fuel flow initially undershoots slightly, but the effective exhaust-nozzle area decreases in the same manner as with the uncompensated systems. The surge problem is thus improved because of the nature of the fuel-flow transient. For the completely compensated system, both the fuel flow and the effective exhaust-nozzle area have negligible transient deviations. This fact, coupled with the negligible speed undershoot for the system, means that, even in surge-prone engines, complete compensation eliminates the surge problem during afterburner starts.

The type of control to be used in afterburner starts depends, then, upon the severity of the surge problem in the engine being studied. All five control systems, of which the uncompensated is the least complex,

eliminate temperature overshoot and steady-state errors as control problems. As the complexity of the control is increased by the addition of compensation, the severity of the speed, fuel-flow, and exhaust-nozzle-area transients is decreased, and the surge problem is correspondingly decreased. Complete compensation reduces the transient variations of all the variables to negligible amounts and therefore eliminates all surge problems during an afterburner start.

Lewis Flight Propulsion Laboratory
National Advisory Committee for Aeronautics
Cleveland, Ohio, July 9, 1956

[redacted]

APPENDIX A

SYMBOLS

A	physical exhaust-nozzle area, sq ft
$\Delta A'$	percent change in exhaust-nozzle area, $\Delta A/A_r$
A_{eff}	effective exhaust-nozzle area, sq ft
$\Delta A'_{eff}$	percent change in effective exhaust-nozzle area, $\Delta A_{eff}/A_r$
$A_{eq,b}$	equivalent afterburning effect on exhaust-nozzle area, sq ft
$\Delta A'_{eq,b}$	percent change in equivalent afterburning effect on exhaust-nozzle area, $\Delta A_{eq,b}/A_r$
C	controller matrix
C_{AN}	transfer function of area to speed controller
C_{AT}	transfer function of area to turbine-discharge temperature controller
C_{w_fN}	transfer function of fuel flow to speed controller
C_{w_fT}	transfer function of fuel flow to turbine-discharge temperature controller
$\mathscr{C}$	completely compensated system
c	controlled output matrix
D	engine dynamics matrix
d	load disturbance matrix
e	error matrix
F_j	jet thrust, lb
f	function
H	feedback or sensor matrix
H_N	transfer function of engine speed sensor
H_T	transfer function of turbine-discharge temperature sensor

[redacted]

$\mathscr{H}$ total enthalpy per pound of air flow at exhaust-nozzle throat

h_{w_b} heat added by afterburner fuel flow per pound of air flow

I identity matrix

K_N speed controller gain

K_N^l gain of engine speed to engine fuel-flow loop

K_{NA} engine gain of speed to exhaust-nozzle area $\left(\left.\frac{\partial N}{\partial A}\right|_{w_f,w_b} \times \frac{A_r}{N_r}\right)$

K_{Nw_b} engine gain of speed to afterburner fuel flow $\left(\left.\frac{\partial N}{\partial w_b}\right|_{A,w_f} \times \frac{w_b''}{N_r}\right)$

K_{Nw_f} engine gain of speed to engine fuel flow $\left(\left.\frac{\partial N}{\partial w_f}\right|_{A,w_b} \times \frac{w_{f,r}}{N_r}\right)$

K_T temperature controller gain

K_T^l gain of turbine-discharge temperature to exhaust-nozzle-area loop

K_{TA} engine gain of turbine-discharge temperature to exhaust-nozzle area $\left(\left.\frac{\partial T}{\partial A}\right|_{w_f,w_b} \times \frac{A_r}{T_r}\right)$

K_{TN} engine gain of turbine-discharge temperature to engine speed $\left(\left.\frac{\partial T}{\partial N}\right|_{w_f,A,w_b} \times \frac{N_r}{T_r}\right)$

K_{Tw_b} engine gain of turbine-discharge temperature to afterburner fuel flow $\left(\left.\frac{\partial T}{\partial w_b}\right|_{A,w_f} \times \frac{w_b''}{T_r}\right)$

K_{Tw_f} engine gain of turbine-discharge temperature to engine fuel flow $\left(\left.\frac{\partial T}{\partial w_f}\right|_{A,w_b} \times \frac{w_{f,r}}{T_r}\right)$

M Mach number

m mass flow, lb-sec/ft

[redacted]

N	engine rotor speed, rpm
$\Delta N'$	percent change in engine rotor speed, $\Delta N/N_r$
P	total pressure, lb/sq in.
$\mathscr{P}$	partially compensated system
p	static pressure, lb/sq in.
Q	unbalanced (accelerating) torque, lb-ft
r	reference input matrix
S	engine steady-state matrix
S_{NA}	engine gain K_{NA}
S_{Nw_f}	engine gain K_{Nw_f}
S_{TA}	engine gain K_{TA}
S_{Tw_f}	engine gain K_{Tw_f}
s	Laplacian operator
T	turbine-discharge temperature, $^{\circ}R$
$\Delta T'$	percent change in turbine-discharge temperature, $\Delta T/T_r$
t	time
U(t)	step function
$\mathscr{U}$	uncompensated system
V	velocity of gas, ft/sec
W	servo matrix
w_b	afterburner fuel flow, lb/hr
$\Delta w_b'$	percent change in afterburner fuel flow, $\Delta w_b/w_b''$
w_f	engine fuel flow, lb/hr
$\Delta w_f'$	percent change in engine fuel flow, $\Delta w_f/w_{f,r}$

CD-4 back

[redacted]

Γ	system characteristic matrix
γ	ratio of specific heats
Δ	change
θ	steady-state coefficient matrix relating controlled outputs to load disturbances
τ_e	engine time constant
φ	steady-state coefficient matrix relating controlled outputs to reference inputs
$\left.\frac{\partial X}{\partial Y}\right\|_Z$	partial derivative of X with respect to Y with Z held constant

Subscripts:

b	with afterburning
d	without afterburning
e	error (reference input - controlled output)
n	exhaust-nozzle throat
r	rated value
s	set (reference) input
t	tailpipe
0	ambient conditions

Superscripts

'	percent
"	value with maximum afterburning

[redacted]

APPENDIX B

NONAFTERBURNING-ENGINE EQUATIONS

The development of the dynamic simulation of the nonafterburning turbojet engine is presented briefly herein. A more complete development is presented in reference 4.

The input or independent variables of the system are engine fuel flow and exhaust-nozzle area. The output or dependent variables considered in this report are engine rotor speed and turbine-discharge temperature. Accelerating torque, the difference between the torque produced by the turbine and the torque absorbed by the compressor, is also considered to account for engine operation at nonequilibrium conditions. The basic assumption of quasi-static operation is used in the development.

Three relations assumed between the engine variables are

$$N = f_1 (w_f, A, Q) \tag{B1}$$

$$T = f_2 (w_f, A, Q) \tag{B2}$$

$$Q = f_3 (w_f, A, N) \tag{B3}$$

From these three relations the following equations are obtained:

$$\Delta N = \left.\frac{\partial N}{\partial w_f}\right|_A \Delta w_f + \left.\frac{\partial N}{\partial A}\right|_{w_f} \Delta A + \frac{\Delta Q}{\left.\frac{\partial Q}{\partial N}\right|_{w_f, A}} \tag{B4}$$

$$\Delta T = \left.\frac{\partial T}{\partial w_f}\right|_A \Delta w_f + \left.\frac{\partial T}{\partial A}\right|_{w_f} \Delta A - \left.\frac{\partial T}{\partial N}\right|_{w_f, A} \left(- \frac{\Delta Q}{\left.\frac{\partial Q}{\partial N}\right|_{w_f, A}} \right) \tag{B5}$$

$$- \frac{\Delta Q}{\left.\frac{\partial Q}{\partial N}\right|_{w_f, A}} = \tau_e \, s \Delta N \tag{B6}$$

The partial derivatives are defined as engine gains, with the indicated variables held constant.

Combining equations (B4) to (B6) yields

$$\Delta N = \left.\frac{\partial N}{\partial w_f}\right|_A \left(\frac{1}{1 + \tau_e s}\right) \Delta w_f + \left.\frac{\partial N}{\partial A}\right|_{w_f} \left(\frac{1}{1 + \tau_e s}\right) \Delta A \tag{B7}$$

$$\Delta T = \left[\left.\frac{\partial T}{\partial w_f}\right|_A - \left.\frac{\partial T}{\partial N}\right|_{w_f,A} \left.\frac{\partial N}{\partial w_f}\right|_A \left(\frac{\tau_e s}{1 + \tau_e s}\right)\right] \Delta w_f +$$

$$\left[\left.\frac{\partial T}{\partial A}\right|_{w_f} - \left.\frac{\partial T}{\partial N}\right|_{w_f,A} \left.\frac{\partial N}{\partial A}\right|_{w_f} \left(\frac{\tau_e s}{1 + \tau_e s}\right)\right] \Delta A \tag{B8}$$

The Δ values in the preceding equations represent incremental deviations from the steady-state values of the variables.

Equations (B7) and (B8) may be put in a more suitable form for simulation purposes by nondimensionalizing, using rated engine operating values as a basis. Equations (B7) and (B8) then become

$$\Delta N' = K_{Nw_f}\left(\frac{1}{1 + \tau_e s}\right) \Delta w_f' + K_{NA}\left(\frac{1}{1 + \tau_e s}\right) \Delta A' \tag{1}$$

$$\Delta T' = \left[K_{Tw_f} - K_{TN}K_{Nw_f}\left(\frac{\tau_e s}{1 + \tau_e s}\right)\right] \Delta w_f' +$$

$$\left[K_{TA} - K_{TN}K_{NA}\left(\frac{\tau_e s}{1 + \tau_e s}\right)\right] \Delta A' \tag{2}$$

With the exception of K_{TN}, the engine gains in equations (1) and (2) may be evaluated from steady-state data. The gain K_{TN} and the engine time constant τ_e must be evaluated from transient data.

APPENDIX C

AFTERBURNING-ENGINE EQUATIONS

A theoretical analysis of the effects of afterburning on the dynamic behavior of a turbojet engine is presented in reference 4. The applicable features of this analysis are presented and discussed in this appendix.

The responses of engine rotor speed and turbine-discharge temperature to engine fuel flow, exhaust-nozzle area, and afterburner fuel flow, as given in reference 4, are

$$\Delta N' = K_{Nw_f}\left(\frac{1}{1+\tau_e s}\right)\Delta w_f' + K_{NA}\left(\frac{1}{1+\tau_e s}\right)\Delta A' + K_{Nw_b}\left(\frac{1}{1+\tau_e s}\right)\Delta w_b' \tag{3}$$

$$\Delta T' = \left[K_{Tw_f} - K_{TN}K_{Nw_f}\left(\frac{\tau_e s}{1+\tau_e s}\right)\right]\Delta w_f' + \left[K_{TA} - K_{TN}K_{NA}\left(\frac{\tau_e s}{1+\tau_e s}\right)\right]\Delta A' + \left[K_{Tw_b} - K_{TN}K_{Nw_b}\left(\frac{\tau_e s}{1+\tau_e s}\right)\right]\Delta w_b' \tag{4}$$

Comparing equations (3) and (4) with equations (1) and (2) shows that the effects of afterburning introduce an additional term into each of the response equations.

From thermodynamic relations, the following equations were developed in reference 4:

$$\frac{K_{Nw_b}}{K_{NA}} = \frac{K_{Tw_b}}{K_{TA}} = -\frac{h_{w_b}}{2\mathscr{H}} \tag{C1}$$

$$1 - \frac{K_{TN}K_{NA}}{K_{TA}} = 1 - \frac{K_{TN}K_{Nw_b}}{K_{Tw_b}} \tag{C2}$$

If the following substitutions are now made:

$$\frac{\Delta A_{eq,b}}{A_r} = \Delta A'_{eq,b} = -\frac{h_{w_b}}{2\mathscr{H}}\left(\frac{\Delta w_b}{w_b''}\right) \tag{C3}$$

$$\frac{\Delta A_{eff}}{A_r} = \frac{\Delta A}{A_r} + \frac{\Delta A_{eq,b}}{A_r} \tag{C4}$$

[redacted]

equations (3) and (4) become

$$\Delta N' = K_{Nw_f}\left(\frac{1}{1+\tau_e s}\right)\Delta w_f' + K_{NA}\left(\frac{1}{1+\tau_e s}\right)\Delta A_{eff}' \tag{5}$$

$$\Delta T' = \left[K_{Tw_f} - K_{TN}K_{Nw_f}\left(\frac{\tau_e s}{1+\tau_e s}\right)\right]\Delta w_f' + \left[K_{TA} - K_{TN}K_{NA}\left(\frac{\tau_e s}{1+\tau_e s}\right)\right]\Delta A_{eff}' \tag{6}$$

Equations (5) and (6) for afterburning operation are now analogous in form to equations (1) and (2) for nonafterburning operation. Afterburner operation may therefore be simulated by considering an effective area A_{eff} rather than the physical exhaust-nozzle area A. The effective area A_{eff} is composed of both the physical area A and the variable $A_{eff,b}$ which represents the effect upon engine operation caused by the increase in tailpipe temperature and pressure when the afterburner is lit.

The magnitude of the $A_{eff,b}$ term remains to be evaluated to complete the analysis. The magnitude of the afterburner effects $A_{eff,b}$ when the afterburner is lit is determined by consideration of the thermodynamic relations involved. The ratio of afterburning to nonafterburning thrust is

$$\frac{F_{j,b}}{F_{j,d}} = \frac{m_{n,b}V_{n,b} + A_{n,b}(p_{n,b} - p_0)}{m_{n,d}V_{n,d} + A_{n,d}(p_{n,d} - p_0)} \tag{C5}$$

which may be written as

$$\frac{F_{j,b}}{F_{j,d}} = \frac{A_{n,b}}{A_{n,d}}\left[\frac{\gamma_{n,b}p_{n,b}M_{n,b}^2 + (p_{n,b} - p_0)}{\gamma_{n,d}p_{n,d}M_{n,d}^2 + (p_{n,d} - p_0)}\right] \tag{C6}$$

Since at the exhaust nozzle

$$M_n = \sqrt{\frac{2}{\gamma_n - 1}\left(\frac{p_t}{p_n}\right)^{\frac{\gamma_n - 1}{\gamma_n}} - 1} \tag{C7}$$

considering the exhaust nozzle as choked ($M_n = 1$) gives

$$\frac{p_t}{p_n} = \left(\frac{\gamma_n - 1}{2}\right)^{\frac{\gamma_n}{\gamma_n - 1}} \tag{C8}$$

Now, the assumption is made that

$$P_{t,b} = P_{t,d}$$

(no pressure loss due to burning), and

$$\gamma_{n,b} = \gamma_{n,d}$$

which gives

$$p_{n,b} = p_{n,d}$$

and, therefore,

$$\frac{F_{j,b}}{F_{j,d}} = \frac{A_{n,b}}{A_{n,d}} \tag{8}$$

In a typical afterburner application, the thrust ratio is approximately 1.5, which gives

$$\frac{F_{j,b}}{F_{j,d}} = \frac{A_{n,b}}{A_{n,d}} = 1.5 \tag{C9}$$

For the engine studied in this report, $A_{n,d}$ = 90 percent of rated area (rated area being the turbine-discharge area), and

$$A_{n,b} = 1.5 \times 90 \text{ percent} = 135 \text{ percent} \tag{C10}$$

In the study presented in this report, 135-percent exhaust-nozzle area is taken to be the maximum physical opening of the exhaust nozzle, and the effect of the afterburning is taken to be a 40-percent decrease in effective area ($\Delta A'_{eq,b}$ = -40 percent). The 5-percent safety factor ensures that the rated turbine conditions will not be exceeded in the steady-state afterburning condition.

REFERENCES

1. Boksenbom, Aaron S., and Hood, Richard: General Algebraic Method Applied to Control Analysis of Complex Engine Types. NACA Rep. 980, 1950. (Supersedes NACA TN 1908.)

2. Pack, George J., and Phillips, W. E., Jr.: Analog Study of Interacting and Noninteracting Multiple-Loop Control Systems for Turbojet Engines. NACA Rep. 1212, 1955. (Supersedes NACA TN 3112.)

[redacted]

3. Feder, Melvin S., and Hood, Richard: Analysis for Control Application of Dynamic Characteristics of Turbojet Engine with Tail-Pipe Burning. NACA TN 2183, 1950.

4. Ketchum, J. R., and Craig, R. T.: Simulation of Linearized Dynamics of Gas-Turbine Engines. NACA TN 2826, 1952.

[redacted]

TABLE I. - STABILITY-CONTOUR END POINTS

System	K_T^l for $K_N^l = 0$	K_N^l for $K_T^l = 0$
Uncompensated:		
Proportional	18	39.2
Proportional plus integral	13.1	35.0
Partially compensated:		
Proportional	∞	16.1
Proportional plus integral	∞	9.0
Completely compensated:		
Proportional	∞	∞
Proportional plus integral	∞	∞

TABLE II. - STEADY-STATE COEFFICIENTS

System	θ_{12}	θ_{22}
Uncompensated:		
Proportional	$\frac{0.67}{1 + K_N^l + K_T^l - K_N^l K_T^l}$	$\frac{-0.89\ K_N^l - 0.30}{1 + K_N^l + K_T^l - K_N^l K_T^l}$
Proportional plus integral	0	0
Partially compensated:		
Proportional	$\frac{0.67}{1 + 3K_N^l}$	$\frac{-0.30}{1 + 3K_T^l}$
Proportional plus integral	0	0
Completely compensated:		
Proportional	$\frac{0.67}{1 + 3K_N^l}$	$\frac{-0.30}{1 + 3K_T^l}$
Proportional plus integral	0	0

[redacted]

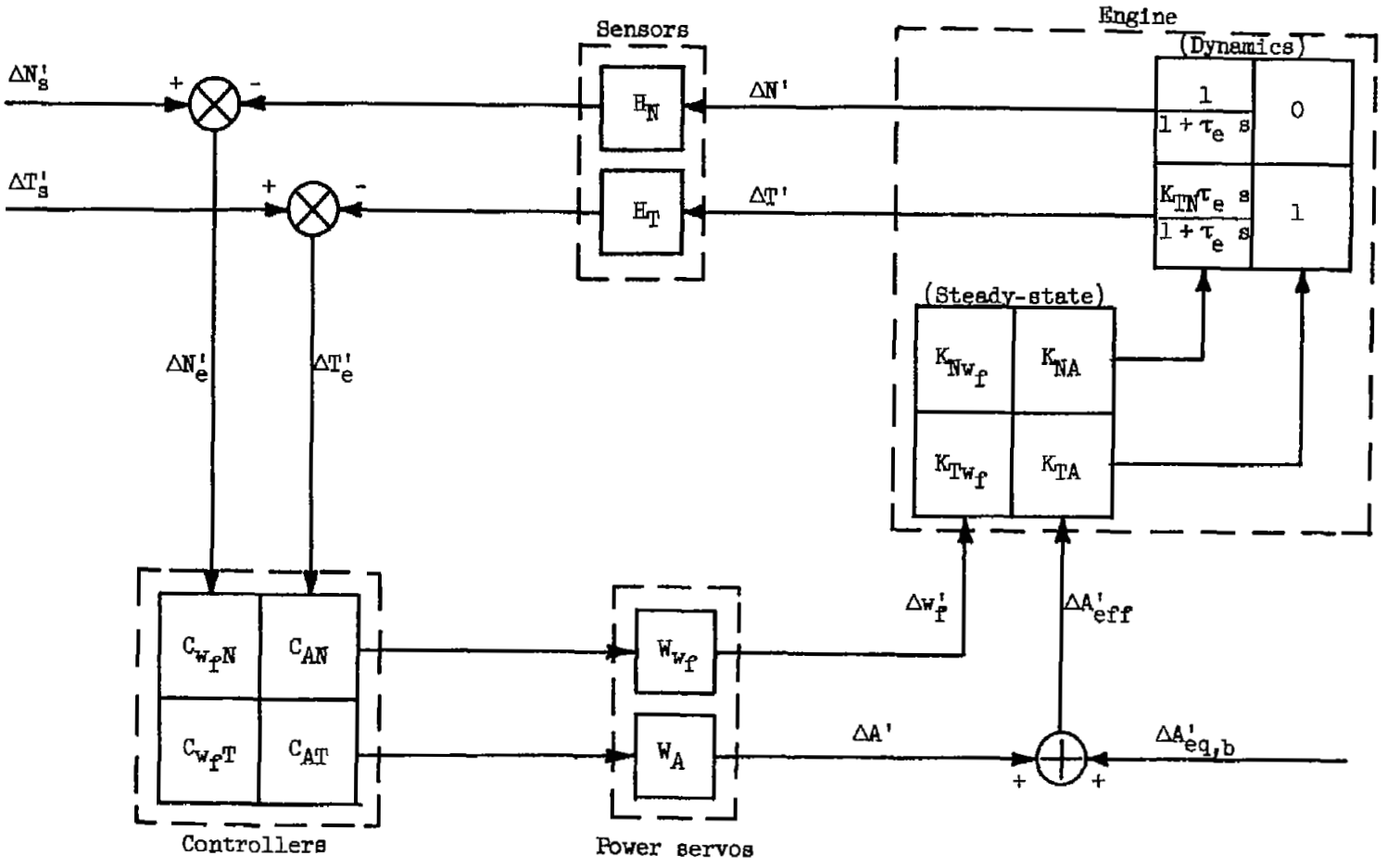

Figure 1. - Block diagram of control system.

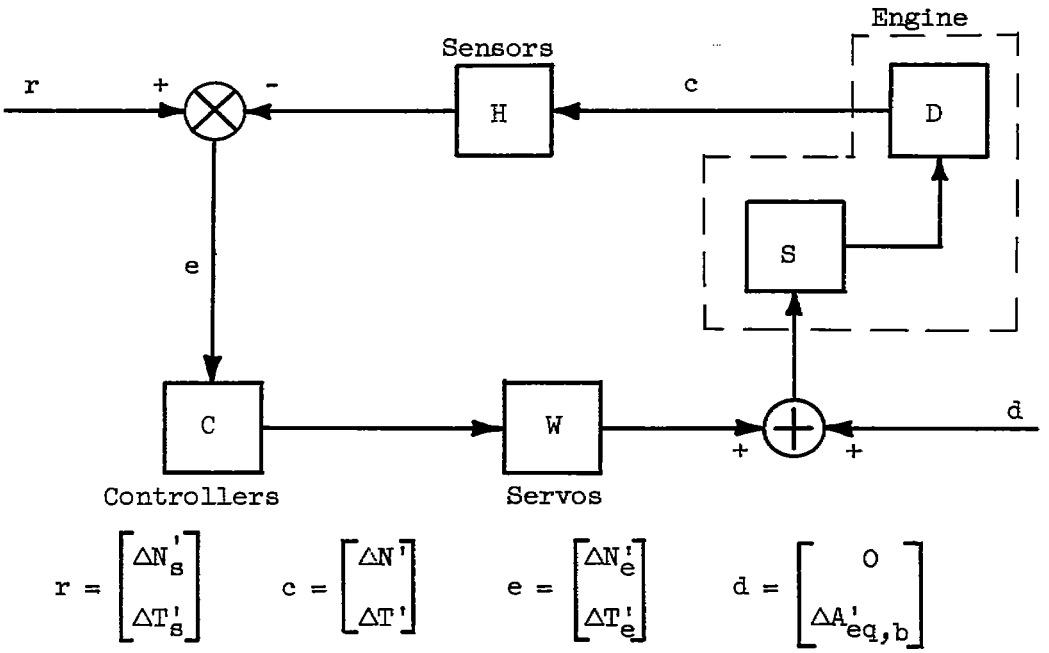

Figure 2. - Matrix diagram of control system.

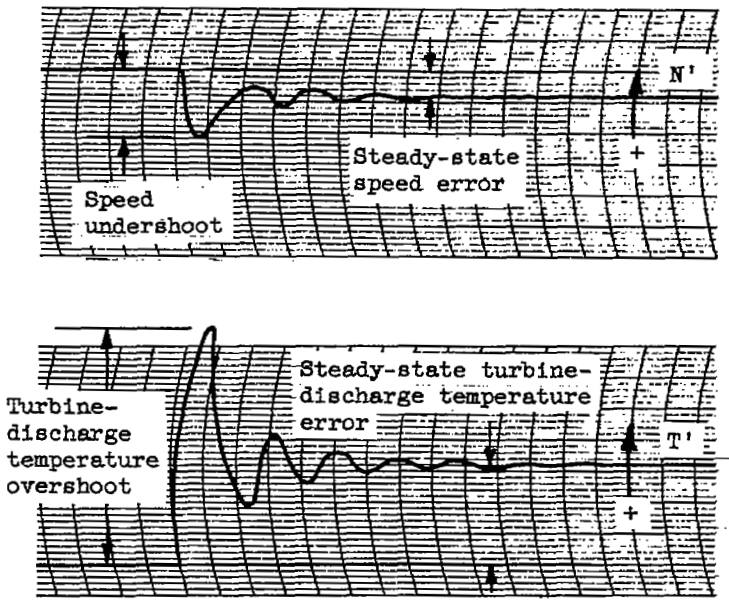

(a) Proportional control.

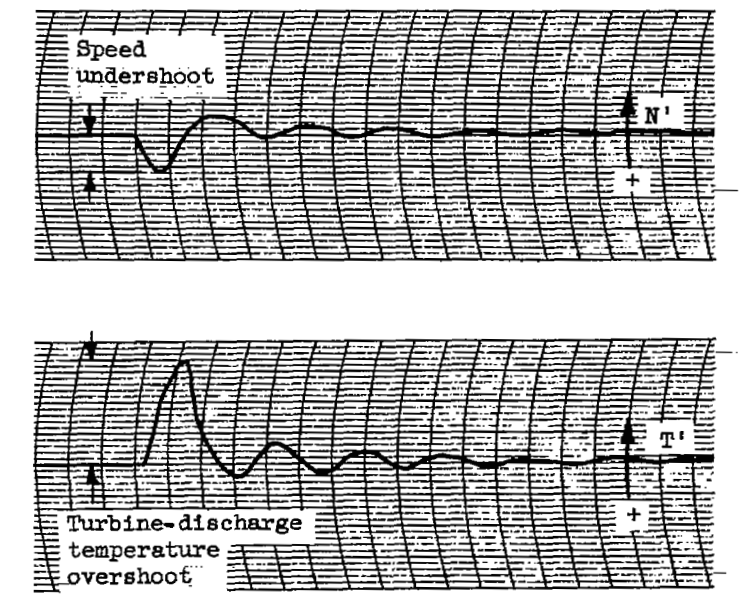

(b) Proportional-plus-integral control.

Figure 3. - Representative traces showing performance criteria considered.

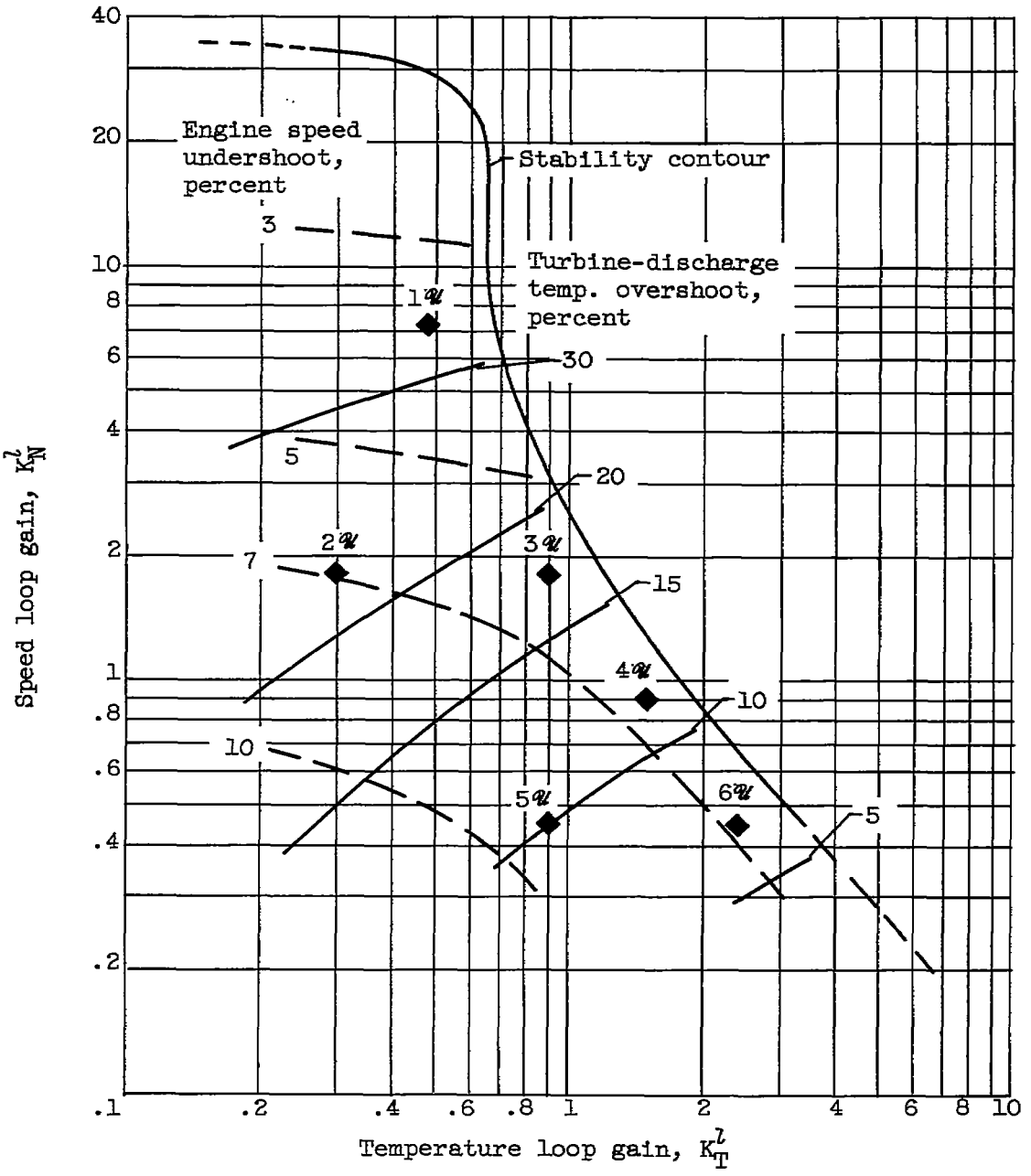

(a) Transient performance.

Figure 4. - Performance criteria for uncompensated proportional-plus-integral system; $\Delta A'_{eq,b} = -40\ U(t)$.

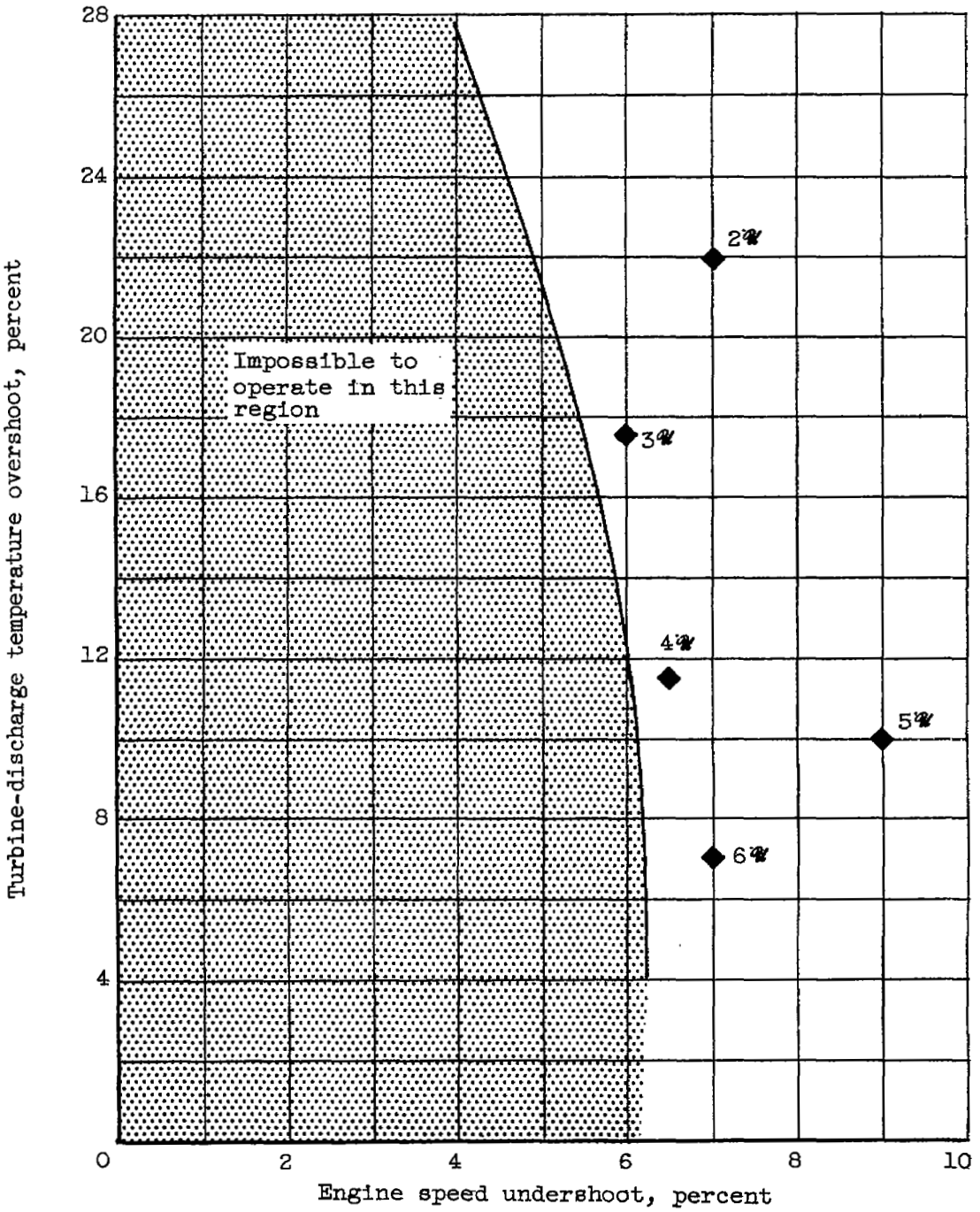

(b) Permissible performance.

Figure 4. - Concluded. Performance criteria for uncompensated proportional-plus-integral system; $\Delta A'_{eq,b} = -40\ U(t)$.

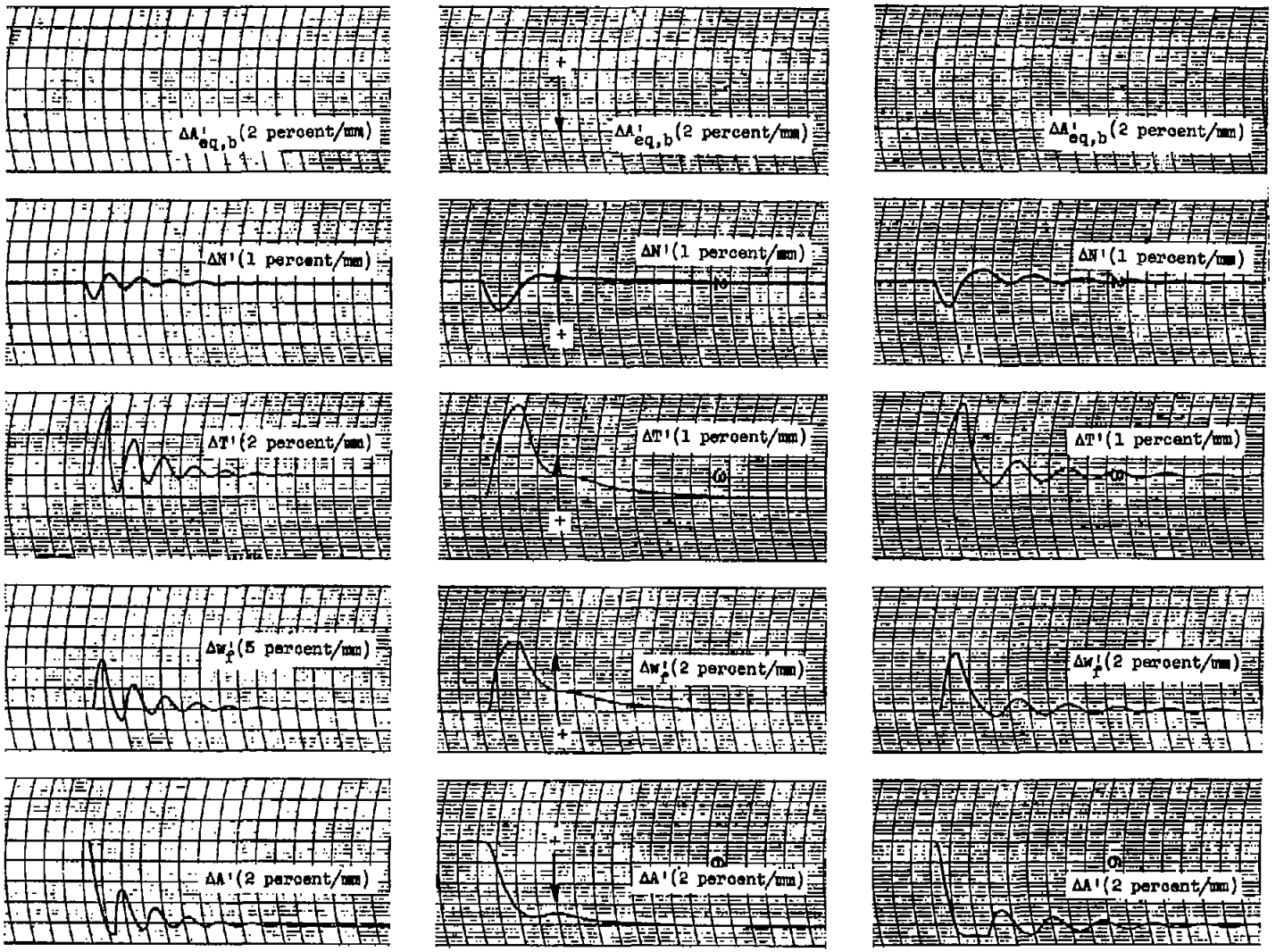

Point 1*: $K'_N = 7.20$; $K'_T = 0.48$.

Point 2*: $K'_N = 1.80$; $K'_T = 0.30$.

Point 3*: $K'_N = 1.80$; $K'_T = 0.90$.

Figure 5. - Analog traces for points 1* to 6* for uncompensated proportional-plus-integral system; $\Delta A'_{eq,b} = -40\ U(t)$.

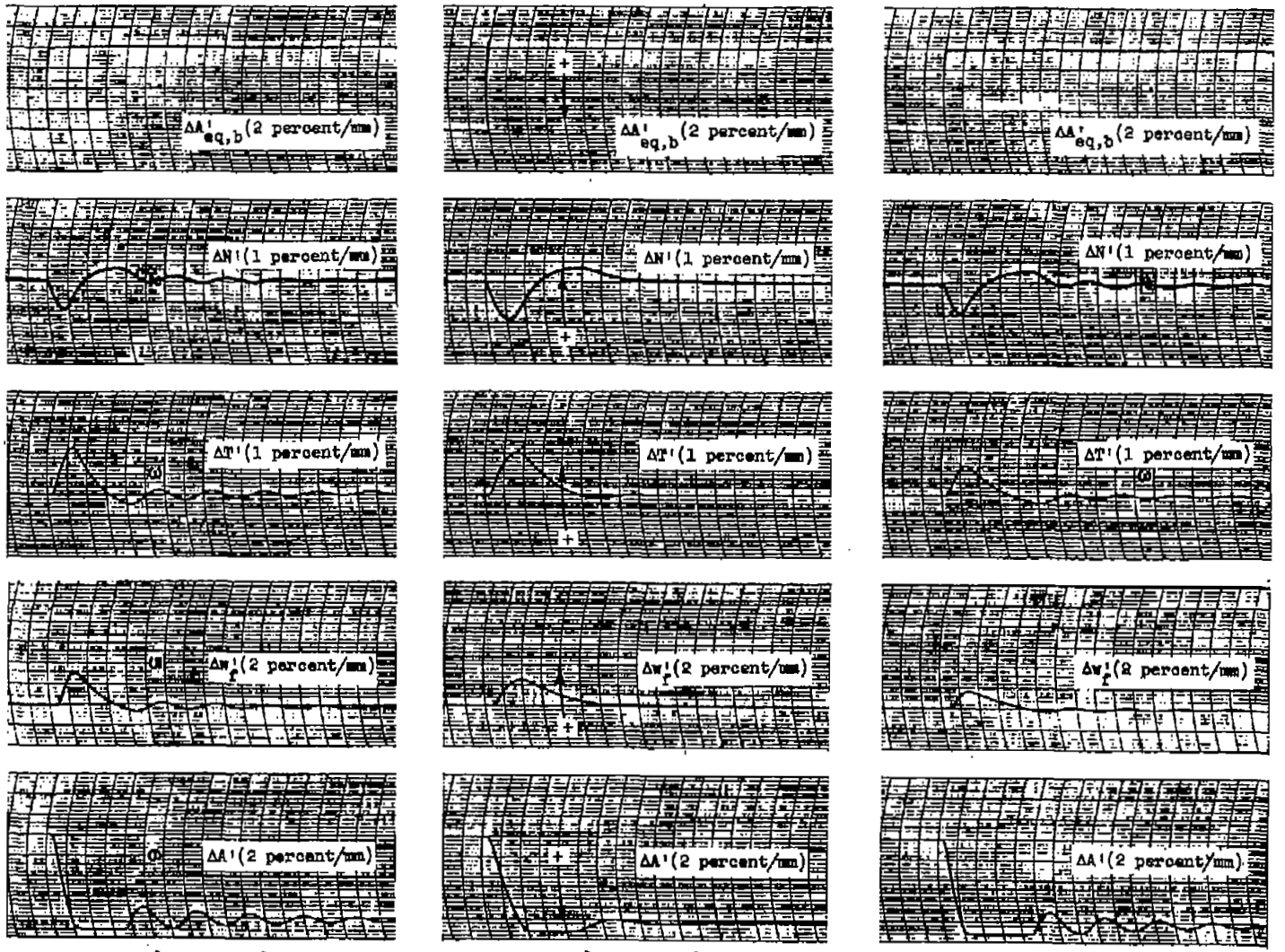

Point 4W: $K_N^1 = 0.90$; $K_T^1 = 1.50$.

Point 5W: $K_N^1 = 0.45$; $K_T^1 = 0.90$.

Point 6W: $K_N^1 = 0.45$; $K_T^1 = 2.4$.

Figure 5. - Concluded. Analog traces for points 1W to 6W for uncompensated proportional-plus-integral system; $\Delta A'_{eq,b} = -40\ U(t)$.

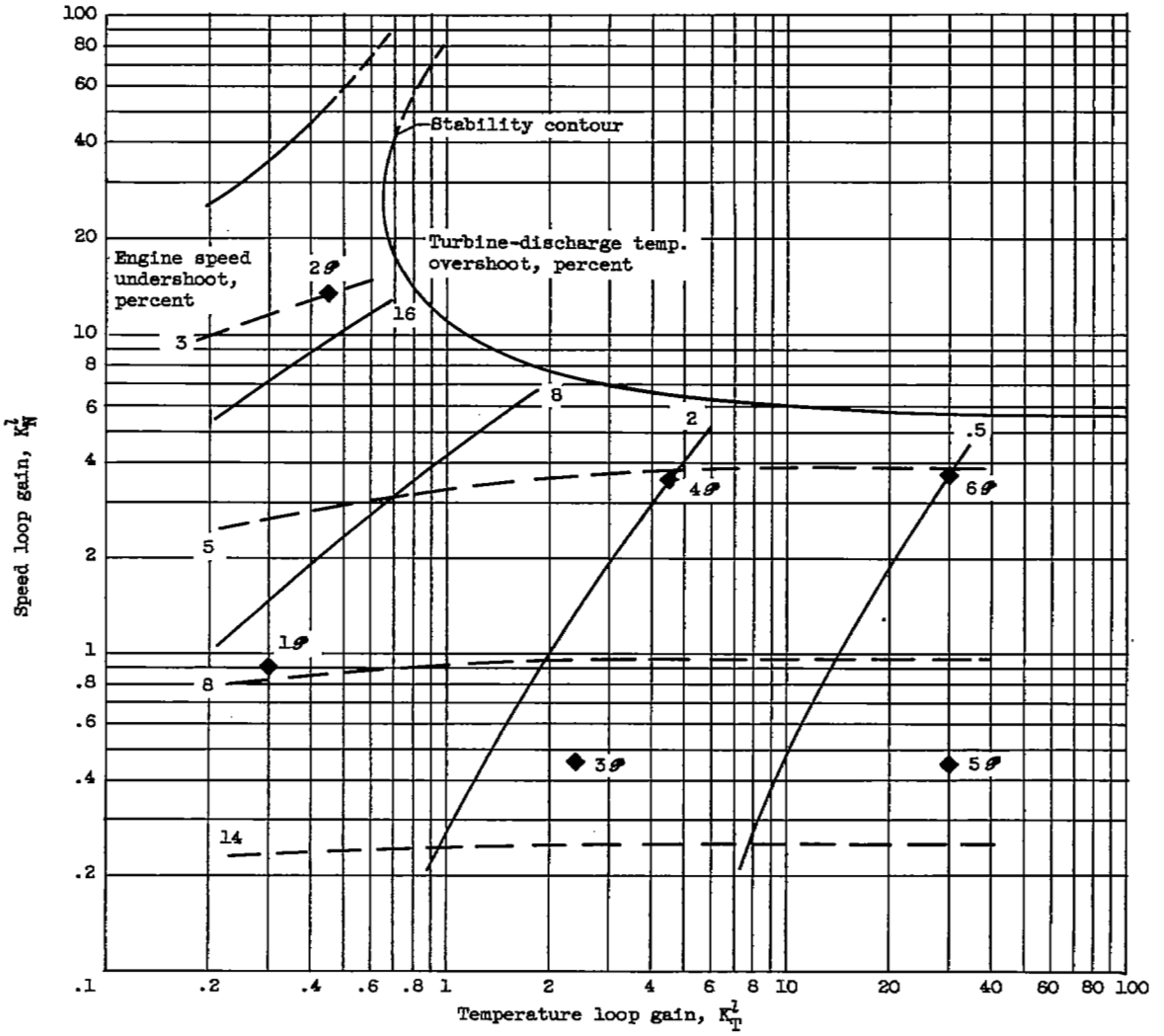

(a) Transient performance.

Figure 6. - Performance criteria for partially compensated proportional system; $\Delta A'_{eq,b} = -40\ U(t)$.

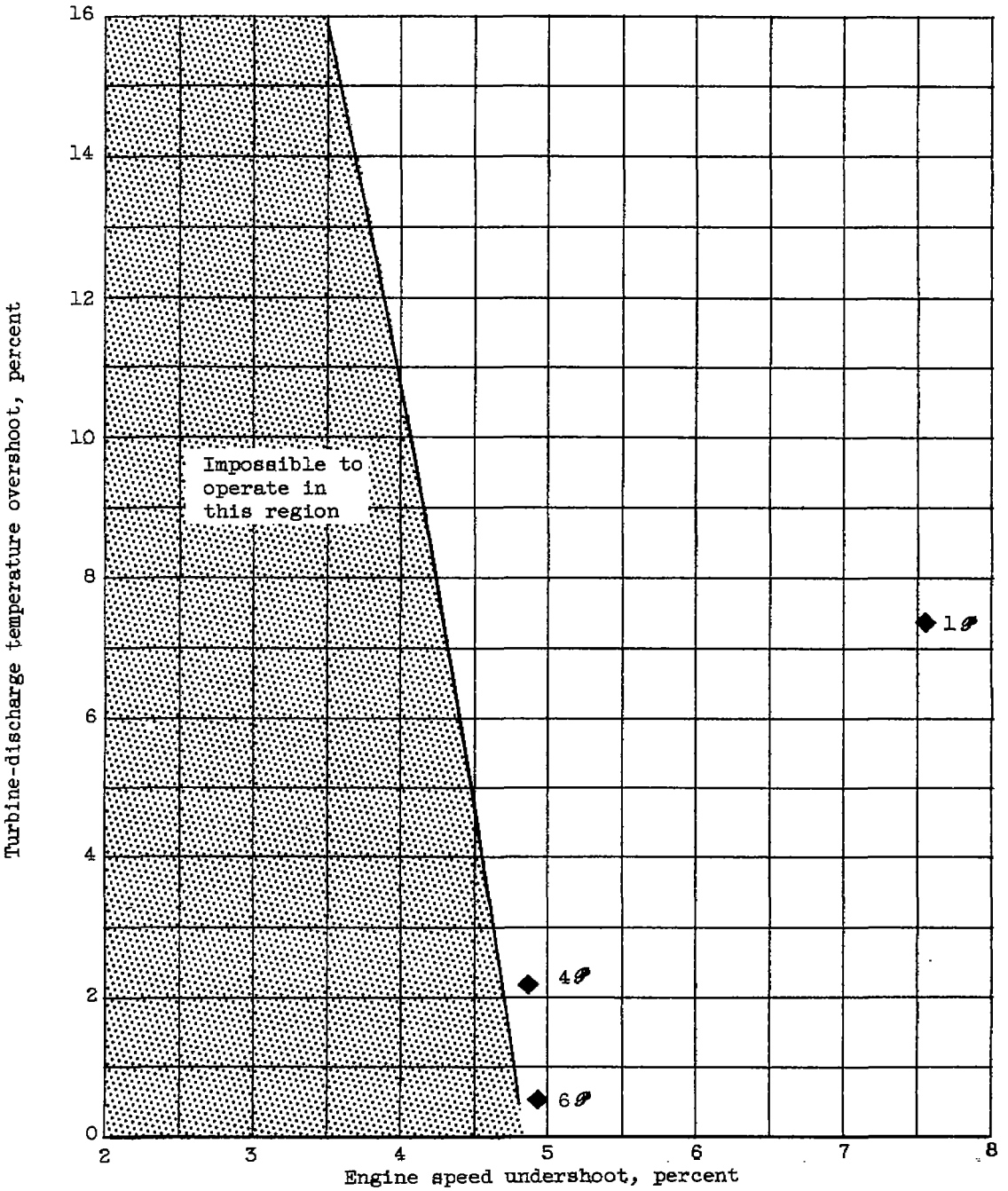

(b) Permissible performance.

Figure 6. - Continued. Performance criteria for partially compensated proportional system; $\Delta A'_{eq,b} = -40\ U(t)$.

[redacted]

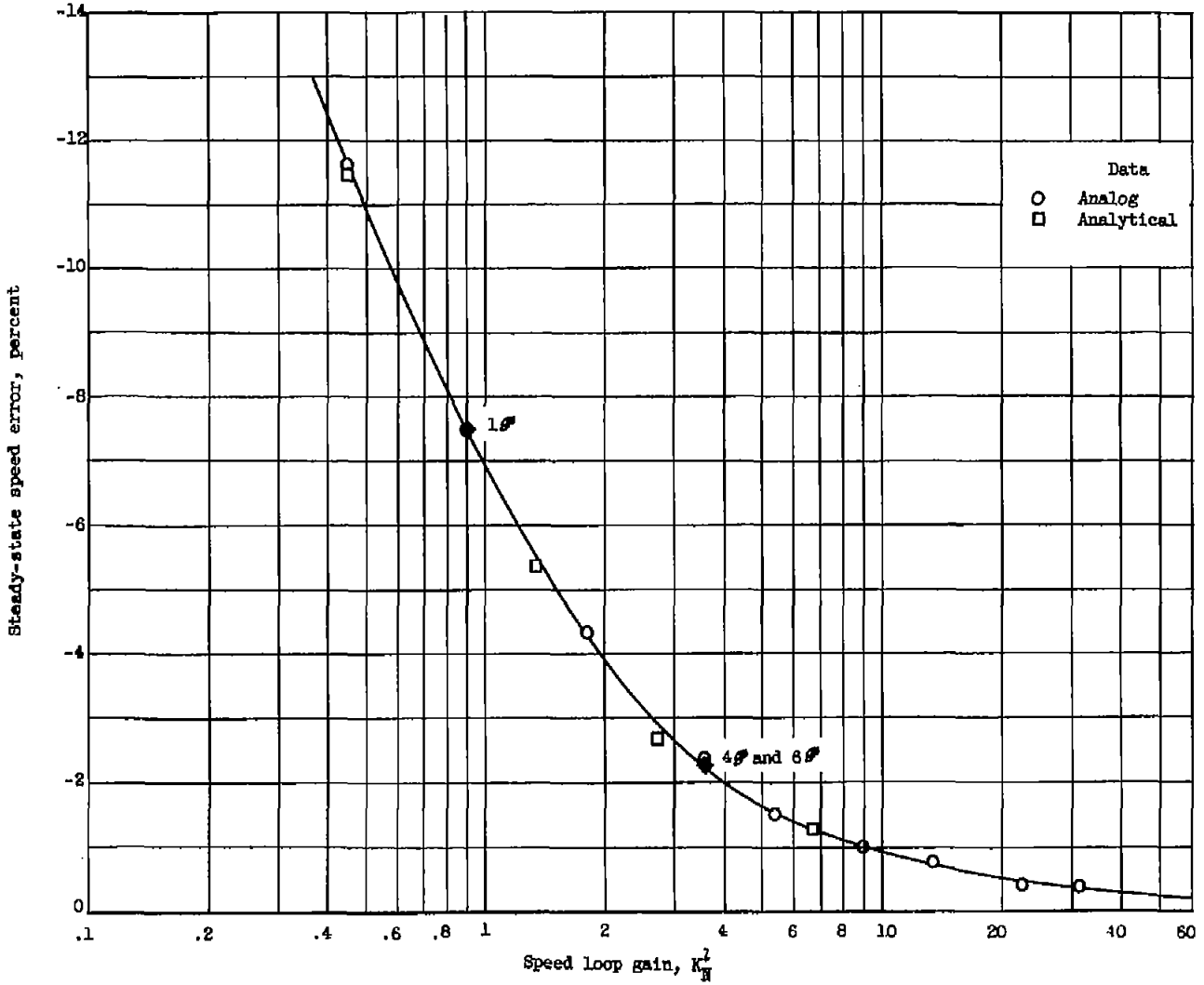

(c) Steady-state speed error.

Figure 6. - Continued. Performance criteria for partially compensated proportional system; $\Delta A'_{eq,b} = -40\ U(t)$.

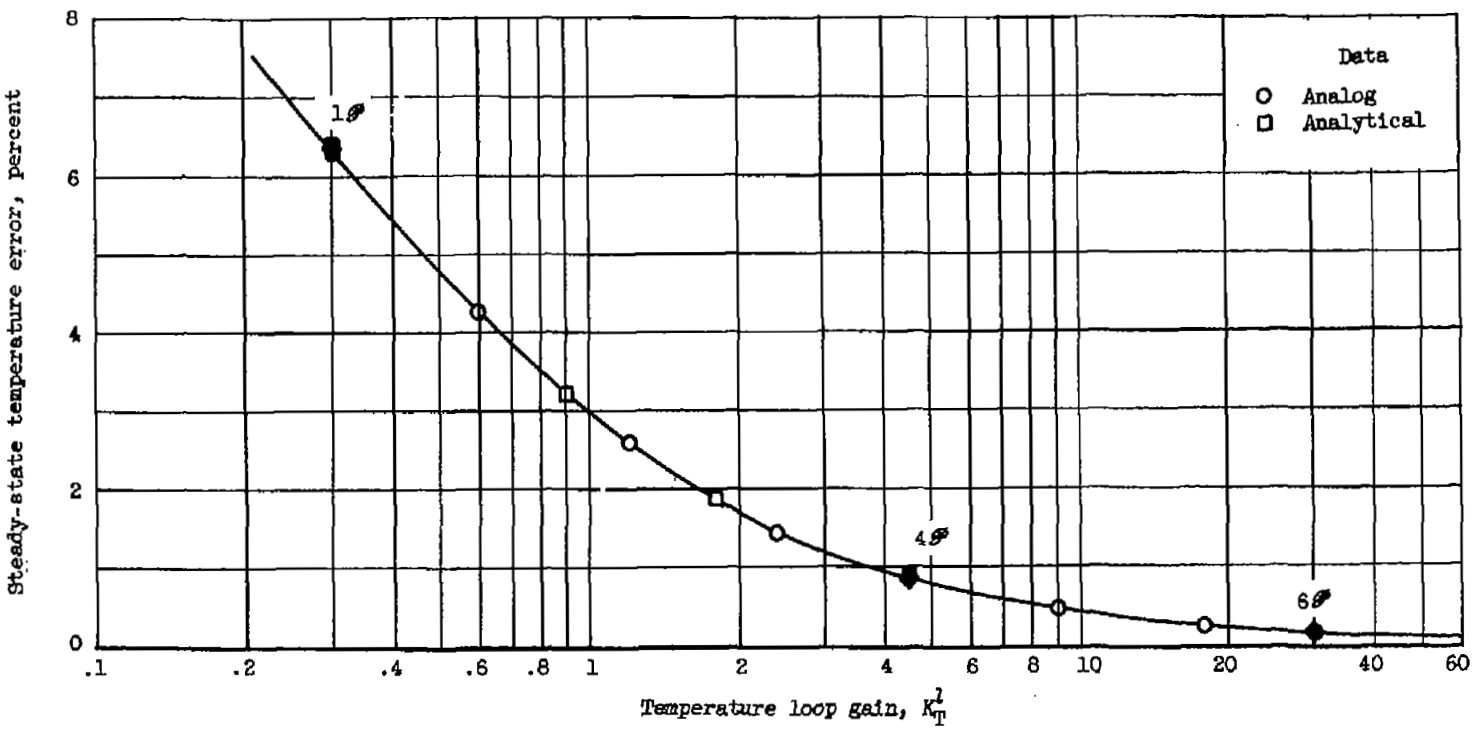

(d) Steady-state temperature error.

Figure 6. - Concluded. Performance criteria for partially compensated proportional system; $\Delta A'_{eq,b} = -40\ U(t)$.

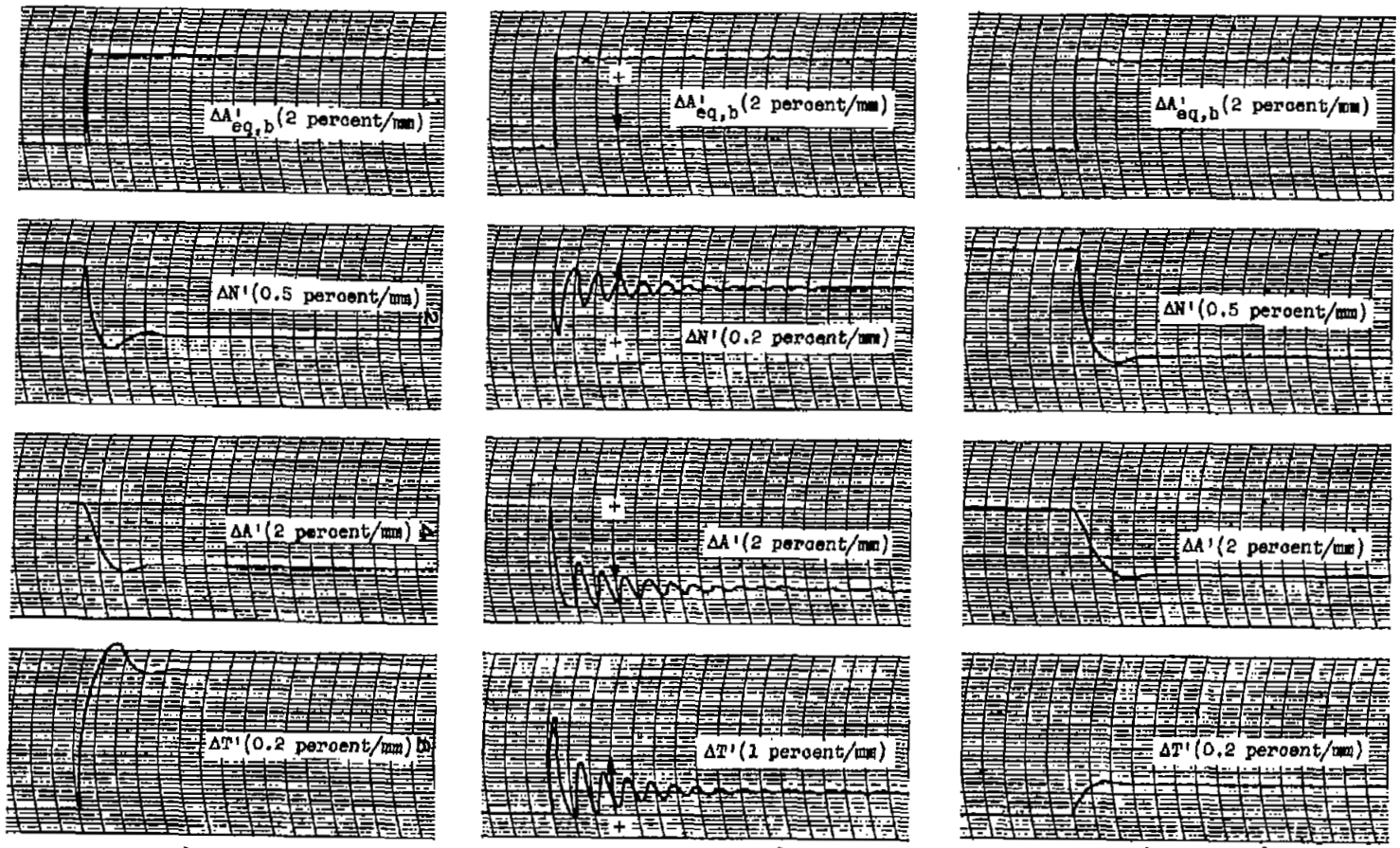

Point 1: $K_N' = 0.90$; $K_T' = 0.30$. Point 2: $K_N' = 13.5$; $K_T' = 0.45$. Point 3: $K_N' = 0.45$; $K_T' = 2.40$.

Figure 7. - Analog traces for points 1 to 6 for partially compensated proportional system; $\Delta A'_{eq,b} = -40\ U(t)$.

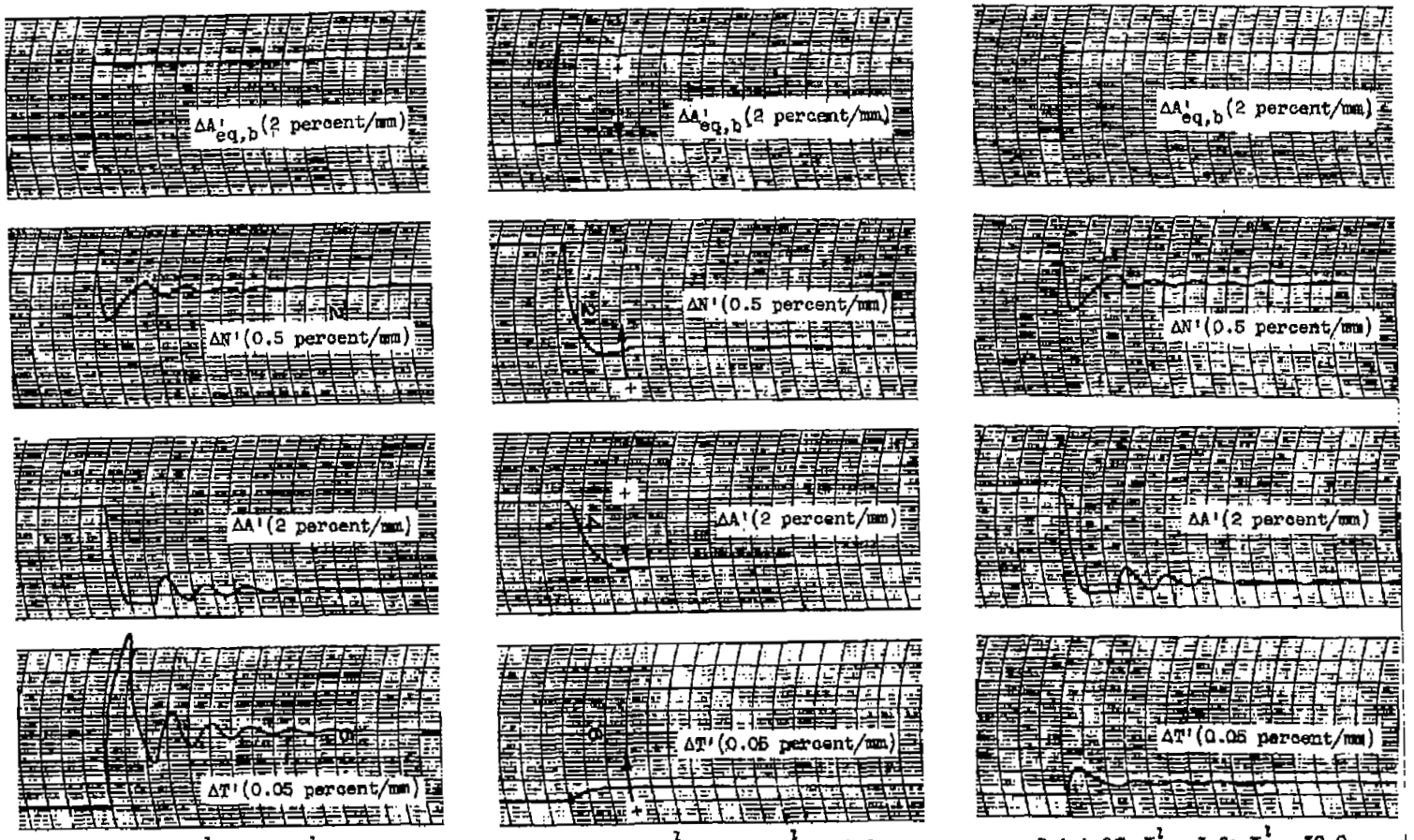

Point 4: $K'_N = 3.8$; $K'_T = 4.5$

Point 5: $K'_N = 0.45$; $K'_T = 30.0$

Point 6: $K'_N = 3.8$; $K'_T = 30.0$

Figure 7. - Concluded. Analog traces for points 1 to 6 for partially compensated proportional system; $\Delta A'_{eq,b} = -40\ U(t)$.

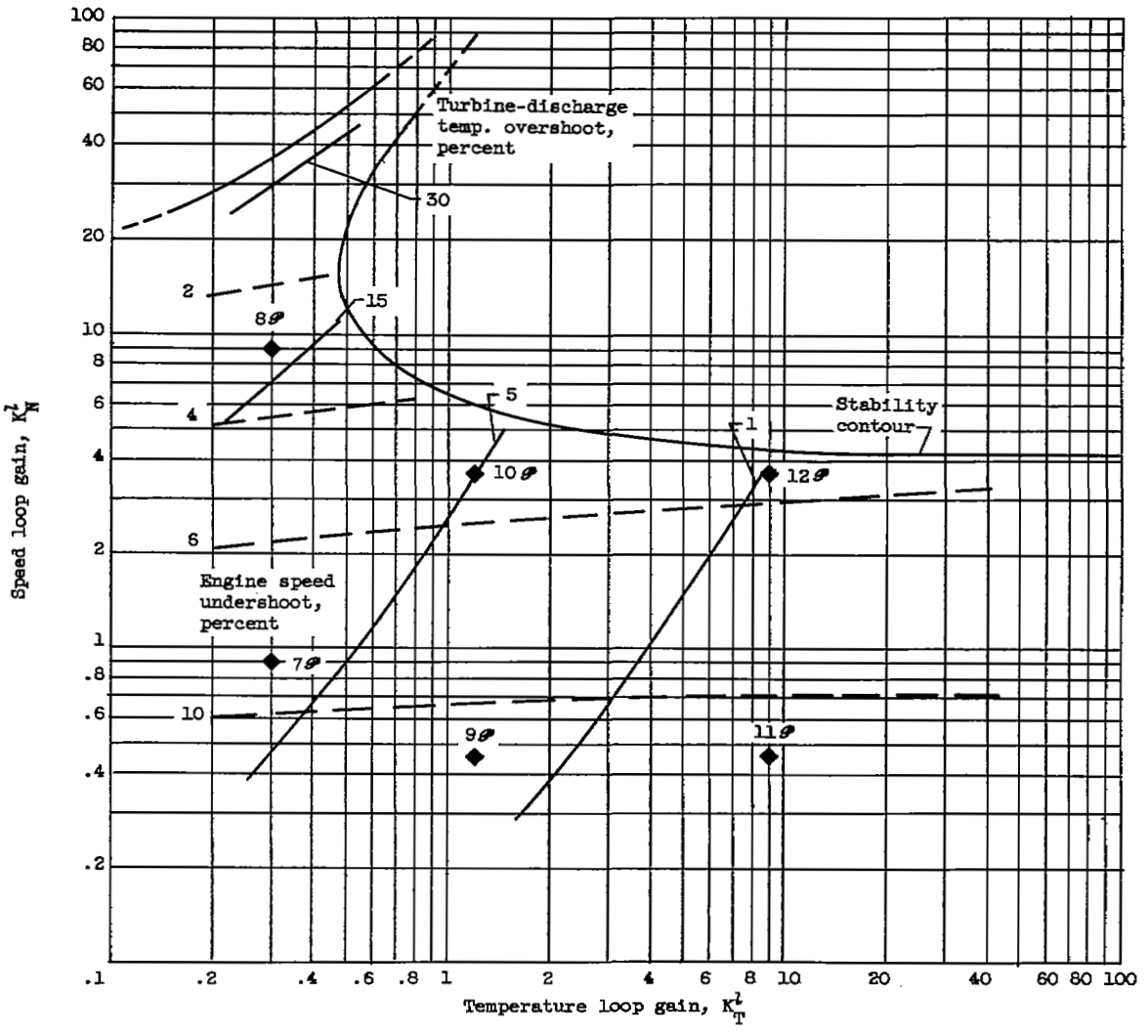

(a) Transient performance.

Figure 8. - Performance criteria for partially compensated proportional-plus-integral system; $\Delta A'_{eq,b} = -40\ U(t)$.

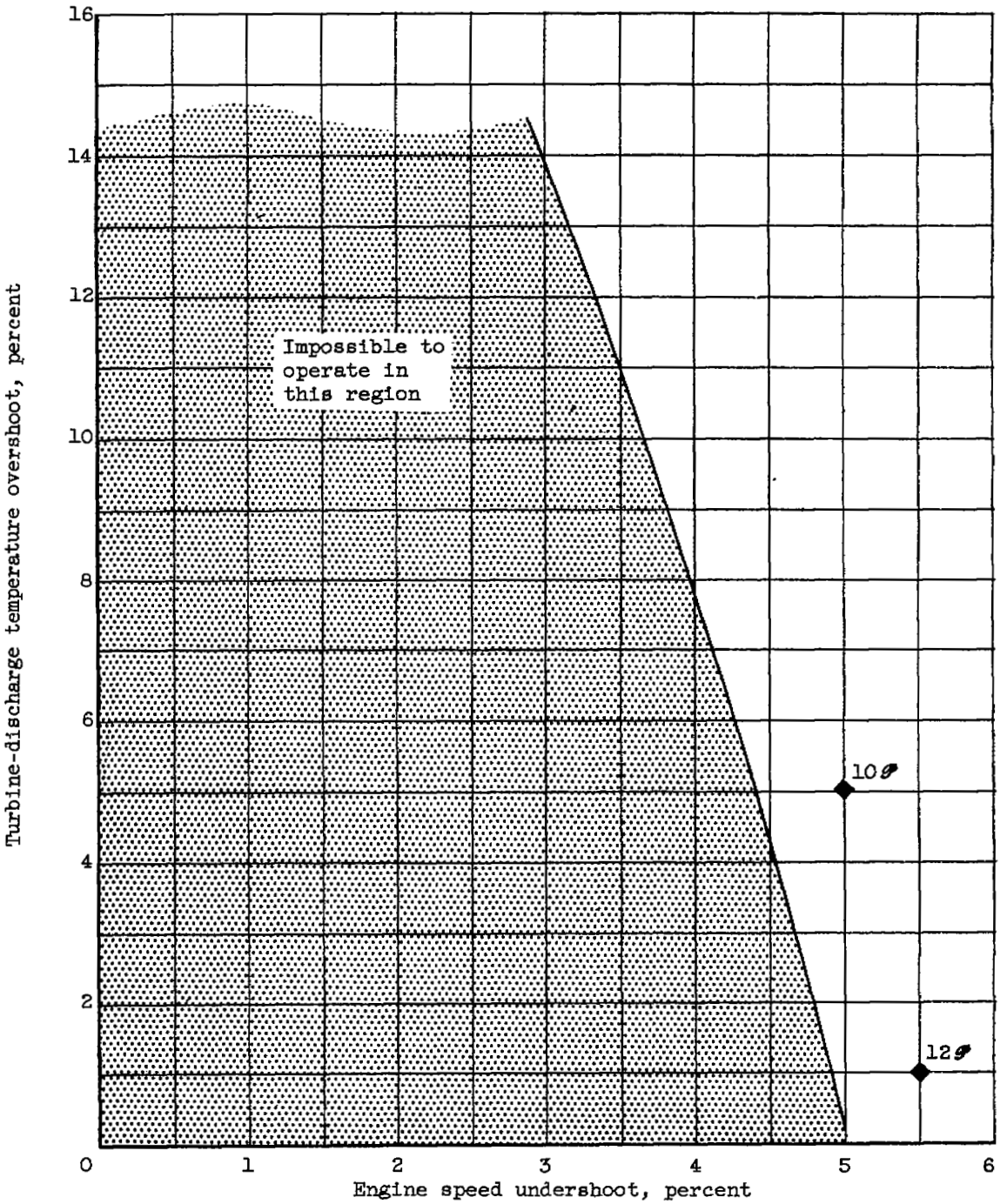

5749

(b) Permissible performance.

Figure 8. - Concluded. Performance criteria for partially compensated proportional-plus-integral system; $\Delta A'_{eq,b} = -40\ U(t)$.

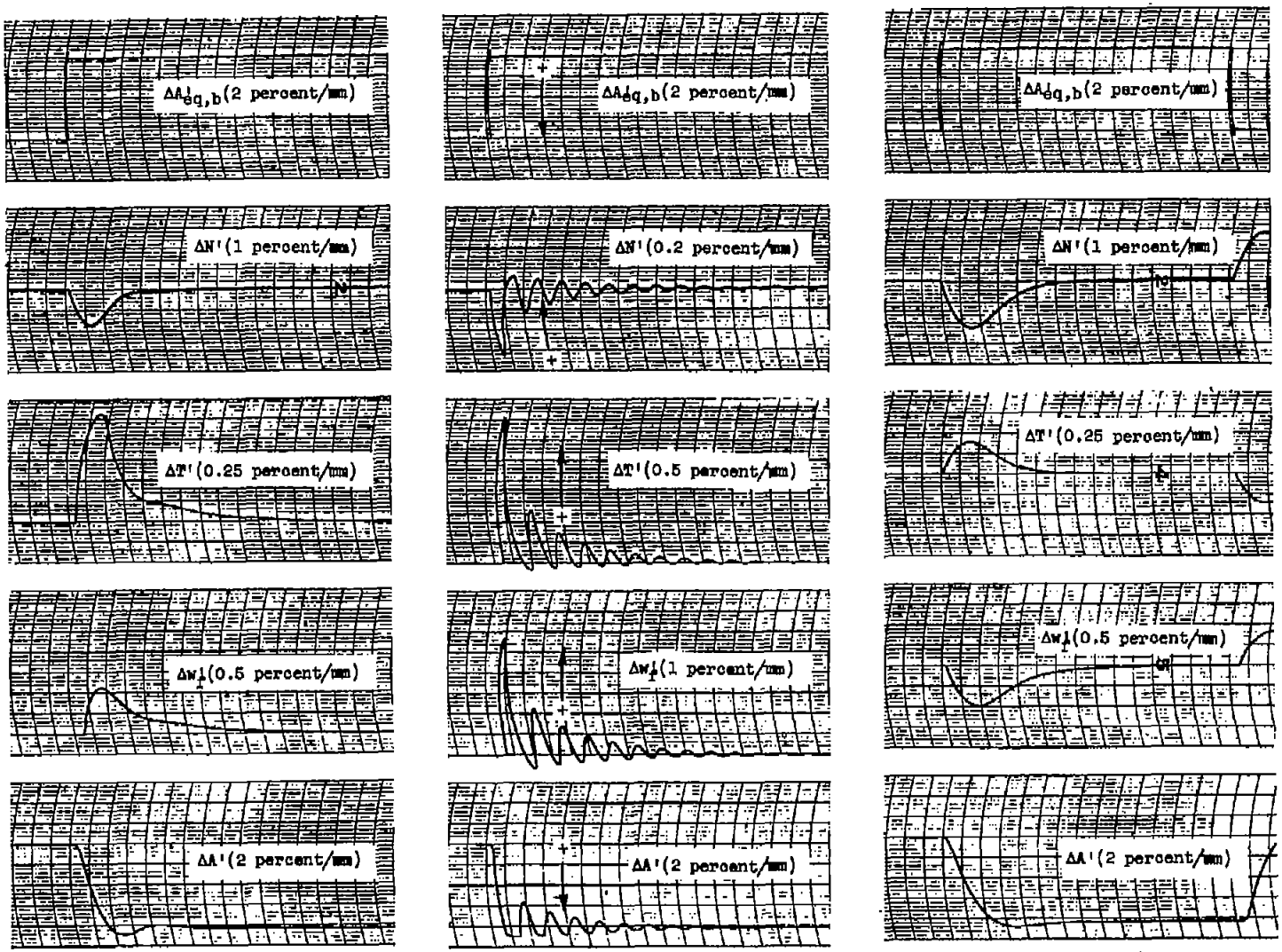

Point 7: $K'_N = 0.90$; $K'_T = 0.30$.

Point 8: $K'_N = 9.0$; $K'_T = 0.30$.

Point 9: $K'_N = 0.45$; $K'_T = 1.20$.

Figure 9. - Analog traces for points 7 to 12 for partially compensated proportional-plus-integral system; $\Delta A'_{eq,b} = -40\ U(t)$.

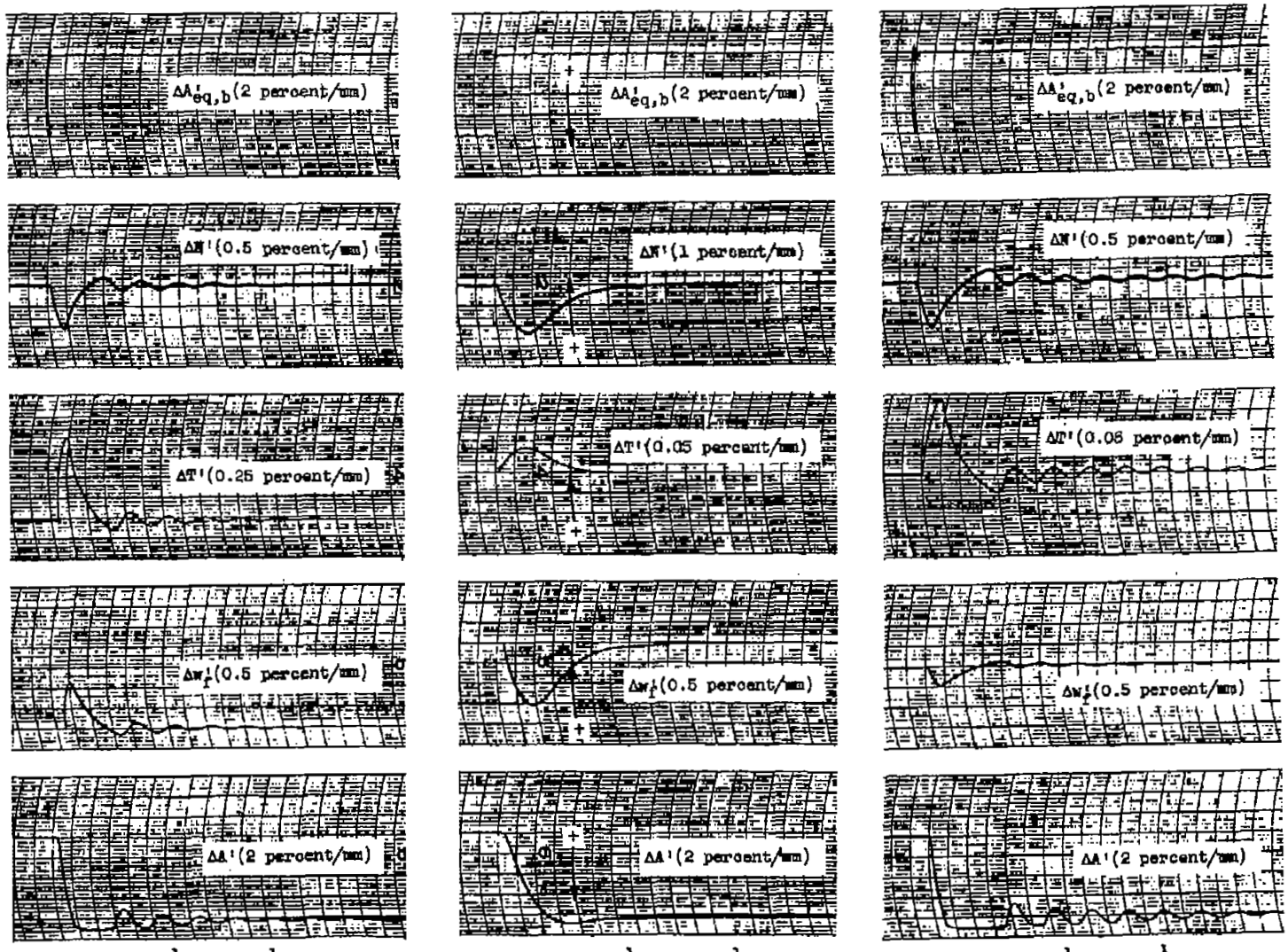

Point 10: $K'_N = 3.6$; $K'_T = 1.2$. Point 11: $K'_N = 0.45$; $K'_T = 4.0$. Point 12: $K'_N = 3.6$; $K'_T = 9.0$.

Figure 9. - Concluded. Analog traces for points 7 to 12 for partially compensated proportional-plus-integral system; $\Delta A'_{eq,b} = -40\ U(t)$.

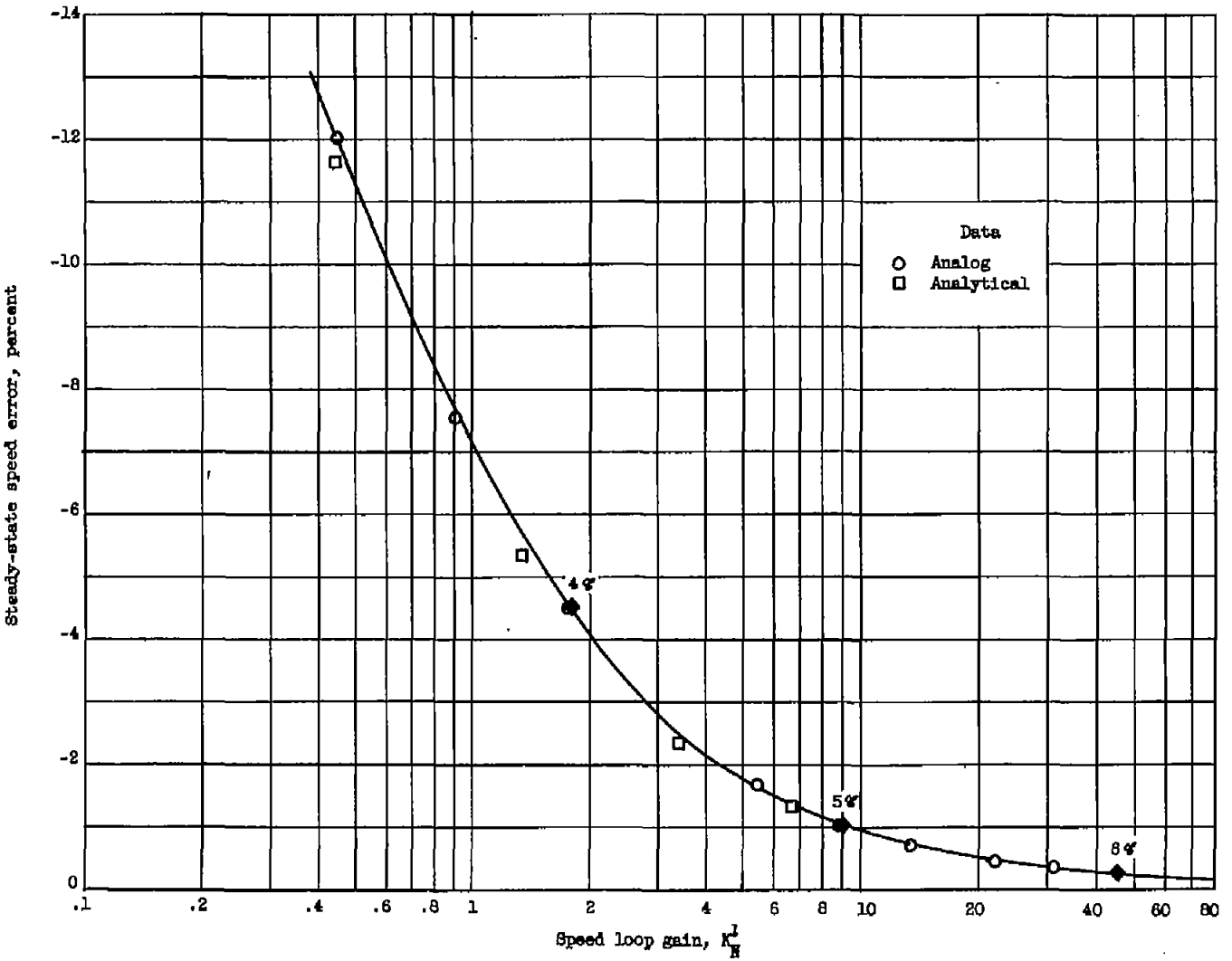

(a) Steady-state speed error.

Figure 10. - Performance criteria for completely compensated proportional system; $\Delta A'_{eq,b} = -40\ U(t)$.

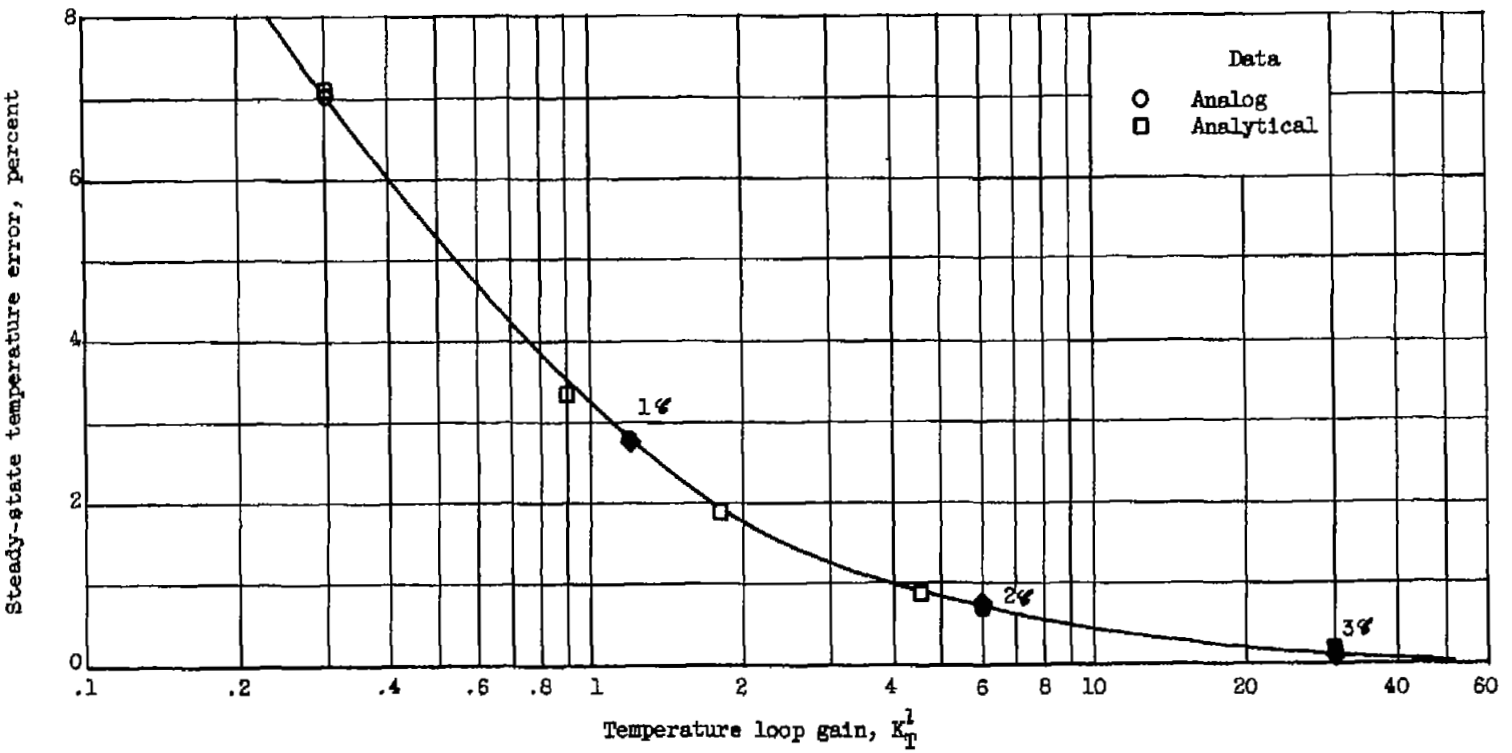

(b) Steady-state temperature error.

Figure 10. - Concluded. Performance criteria for completely compensated proportional system; $\Delta A'_{eq,b} = -40\ U(t)$.

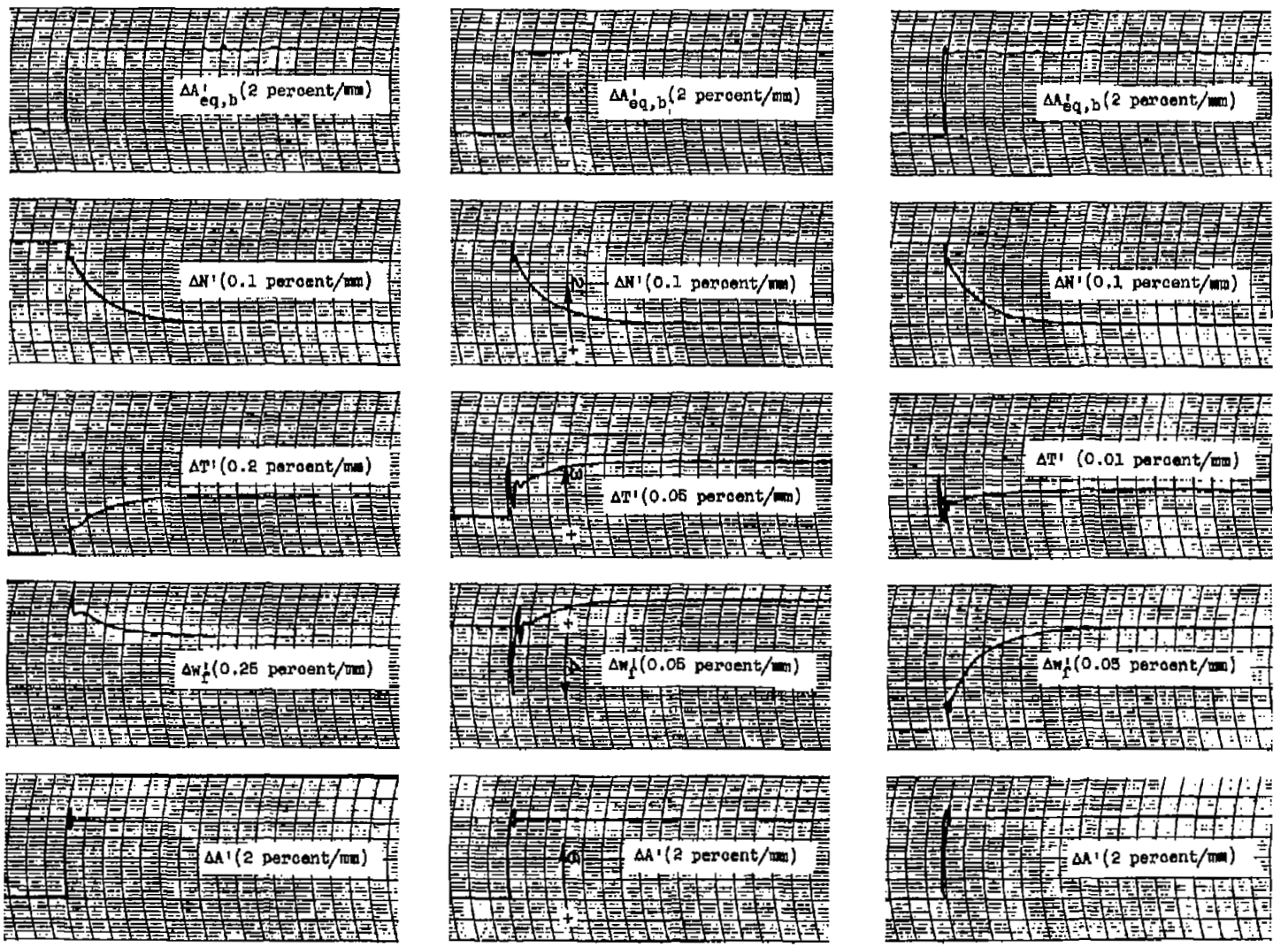

Figure 11. - Analog traces for points 1 to 6 for completely compensated proportional system; $\Delta A'_{eq,b} = -40\ U(t)$.

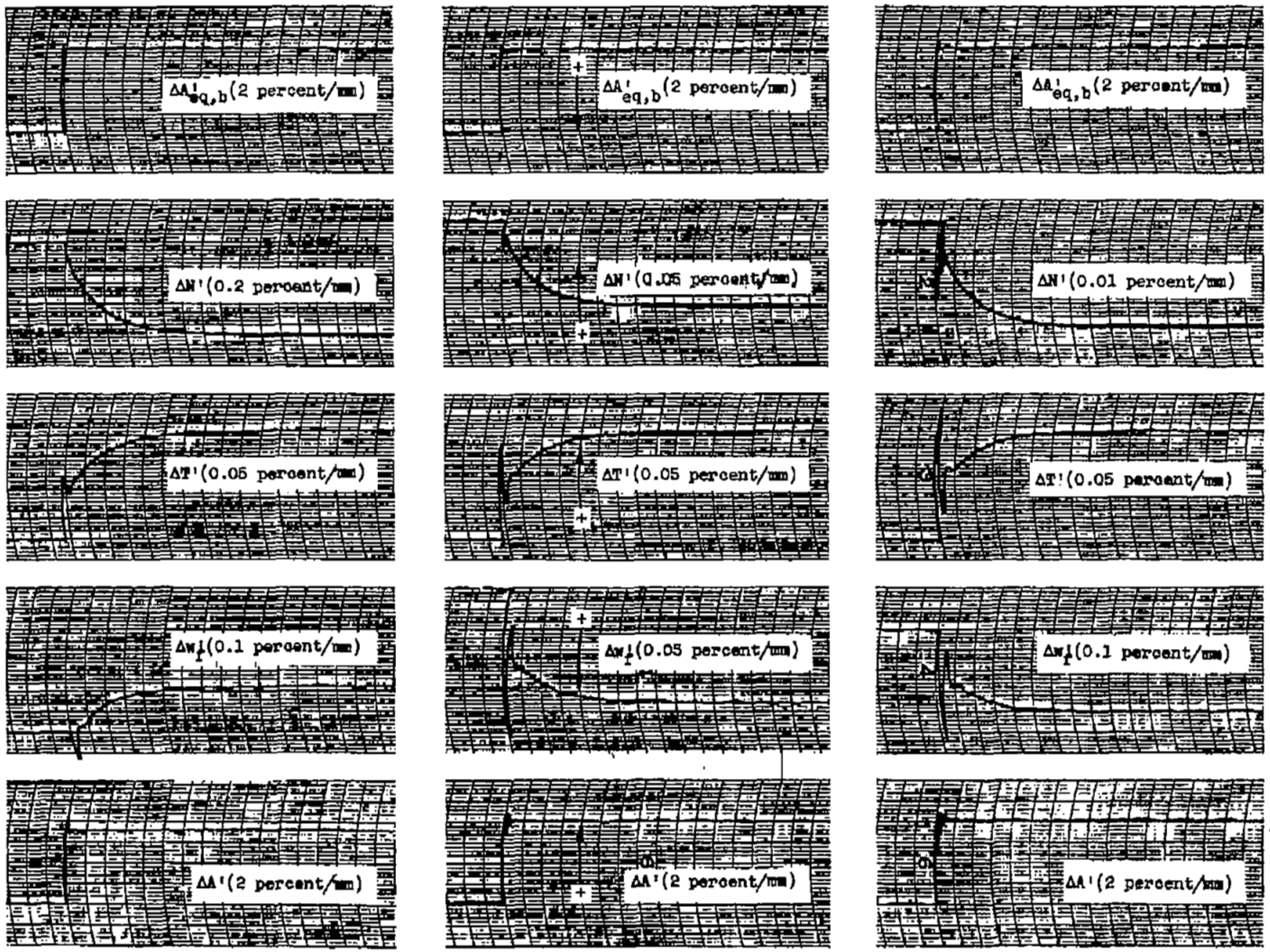

Point 4W: $K_N^1 = 1.80$; $K_T^1 = 3.0$. Point 5W: $K_N^1 = 9.0$; $K_T^1 = 3.0$. Point 6W: $K_N^1 = 45$; $K_T^1 = 3.0$.

Figure 11. - Concluded. Analog traces for points 1W to 6W for completely compensated proportional system; $\Delta A'_{eq,b} = -40\ U(t)$.

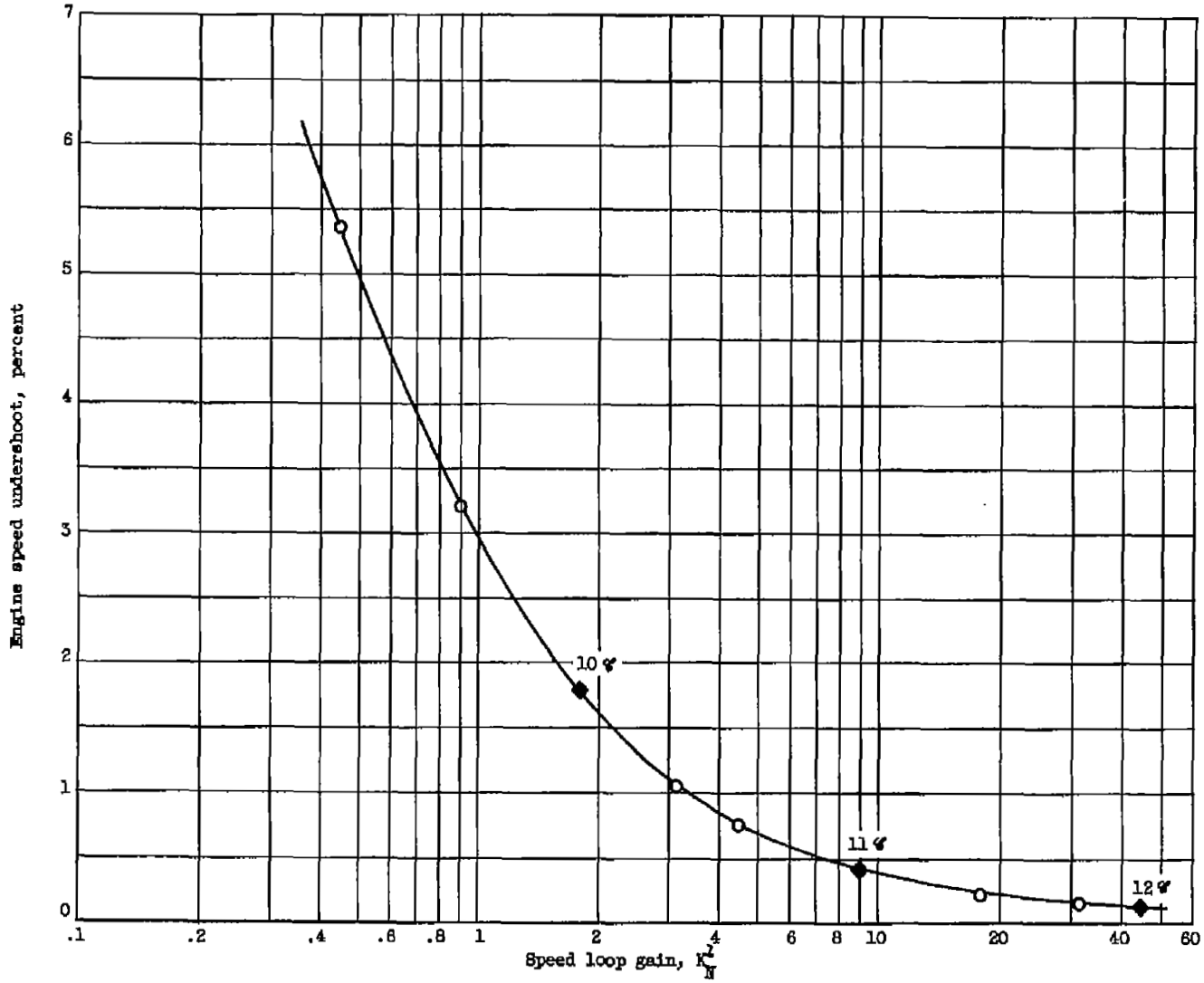

(a) Engine speed undershoot.

Figure 12. - Performance criteria for completely compensated proportional-plus-integral system; $\Delta A'_{eq,b} = -40\ U(t)$.

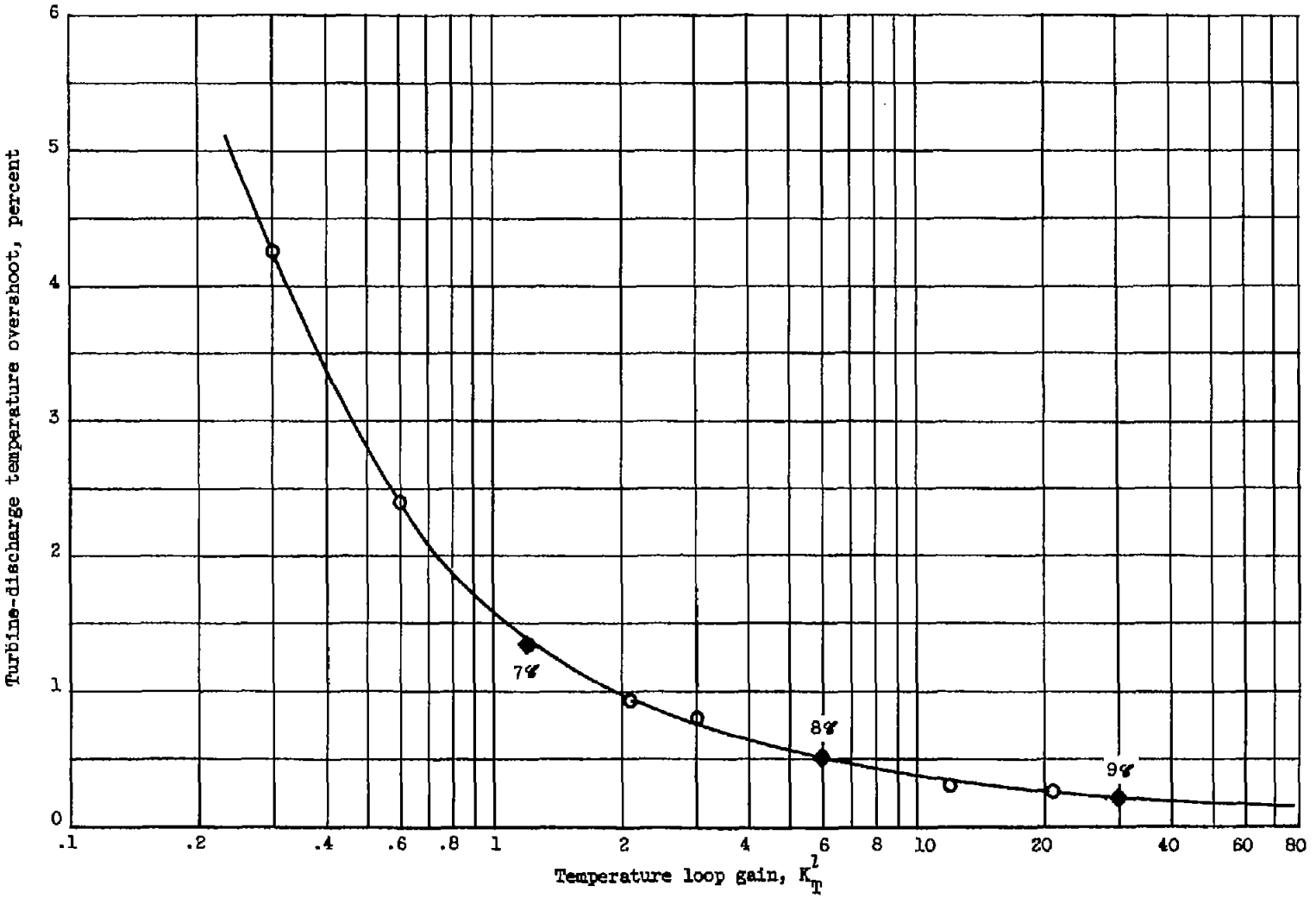

(b) Turbine-discharge temperature overshoot.

Figure 12. - Concluded. Performance criteria for completely compensated proportional-plus-integral system; $\Delta A'_{eq,b} = -40\ U(t)$.

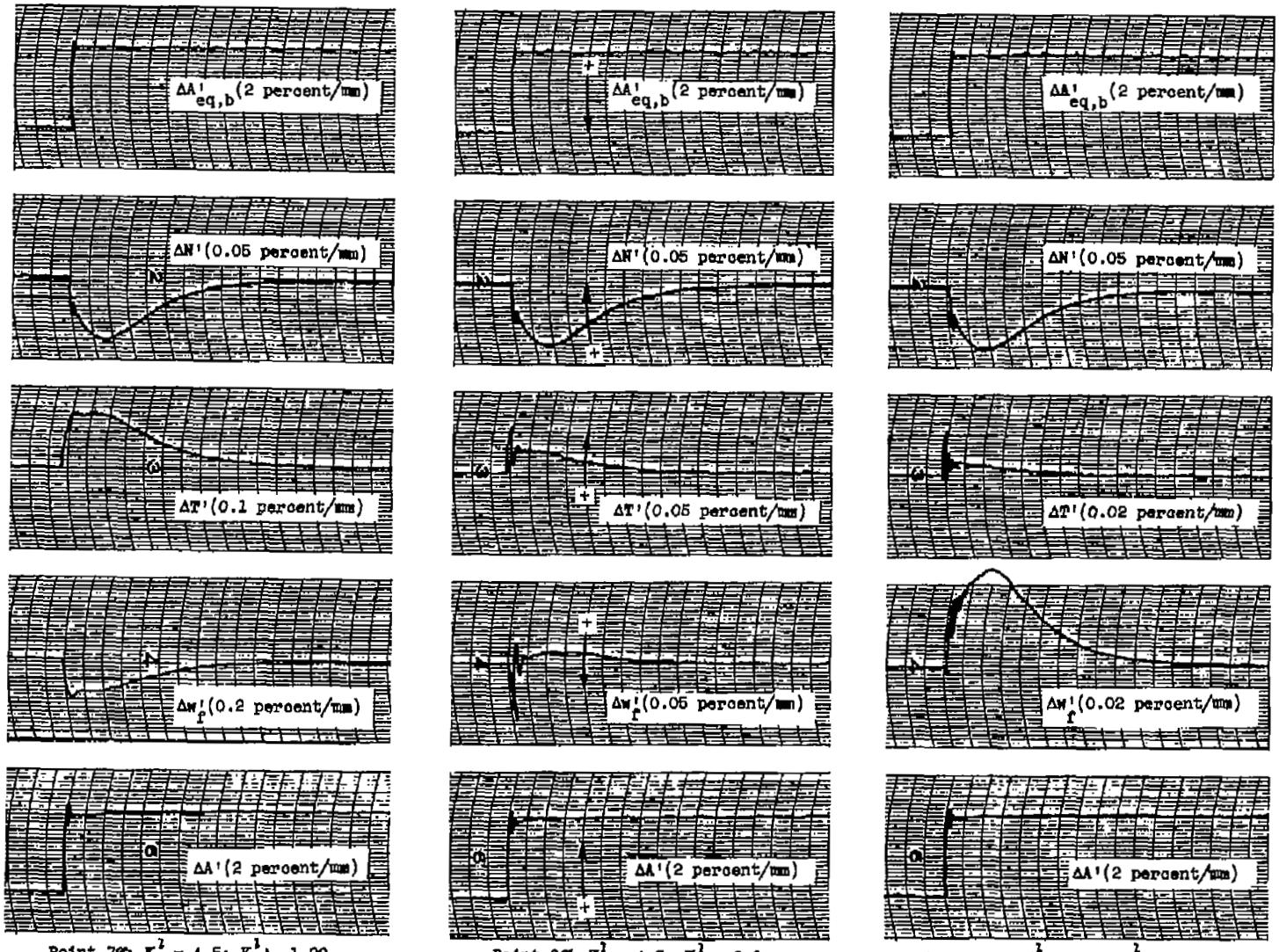

Figure 15. - Analog traces for points 7W to 12W for completely compensated proportional-plus-integral system; $\Delta A'_{eq,b} = -40\ U(t)$.

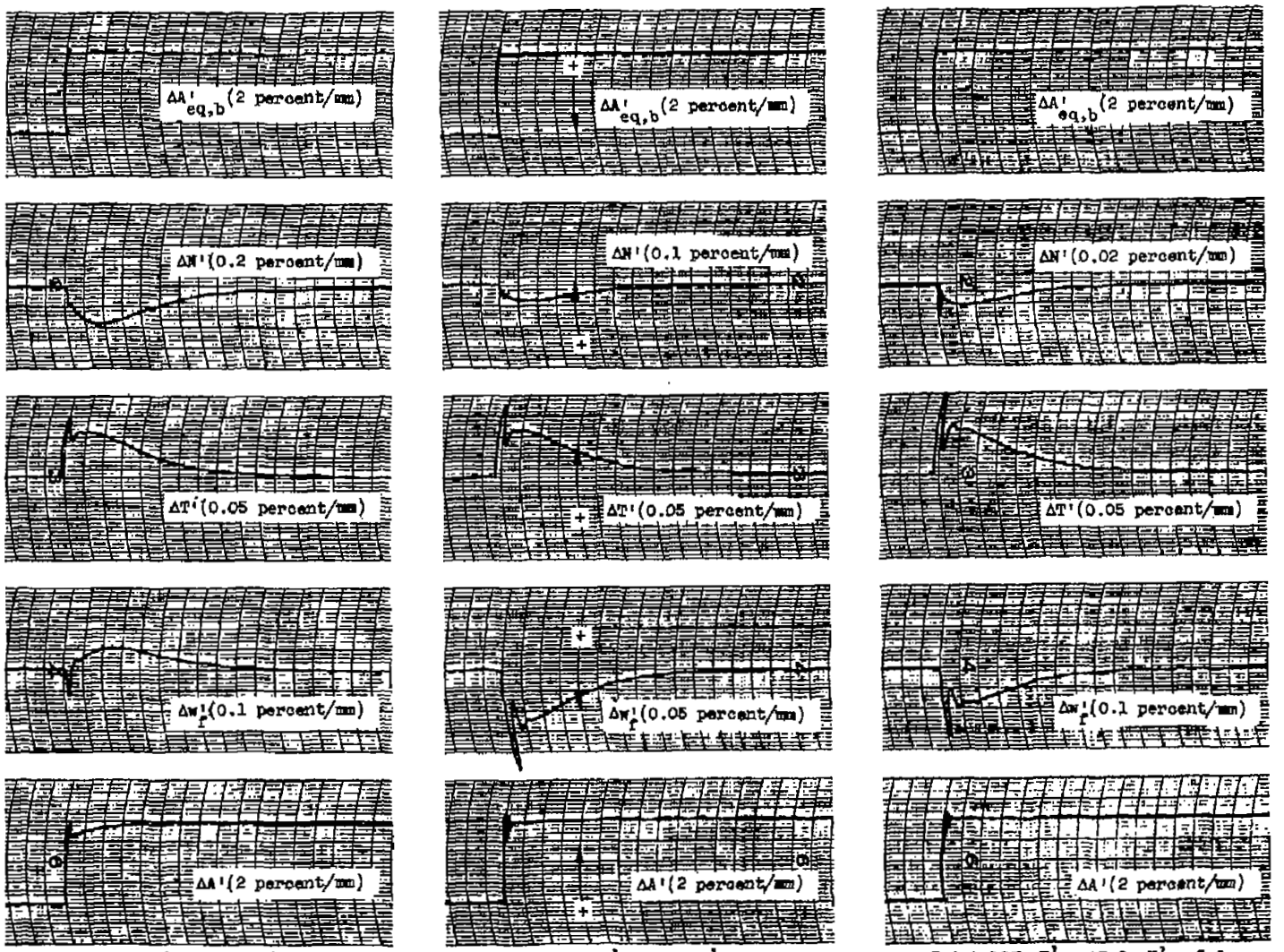

Point 10℉: $K_N^1 = 1.80$; $K_T^1 = 3.0$.

Point 11℉: $K_N^1 = 9.0$; $K_T^1 = 3.0$.

Point 12℉: $K_N^1 = 45.0$; $K_T^1 = 3.0$.

Figure 13. - Concluded. Analog traces for points 7℉ to 12℉ for completely compensated proportional-plus-integral system; $\Delta A'_{eq,b} = -40\ U(t)$.

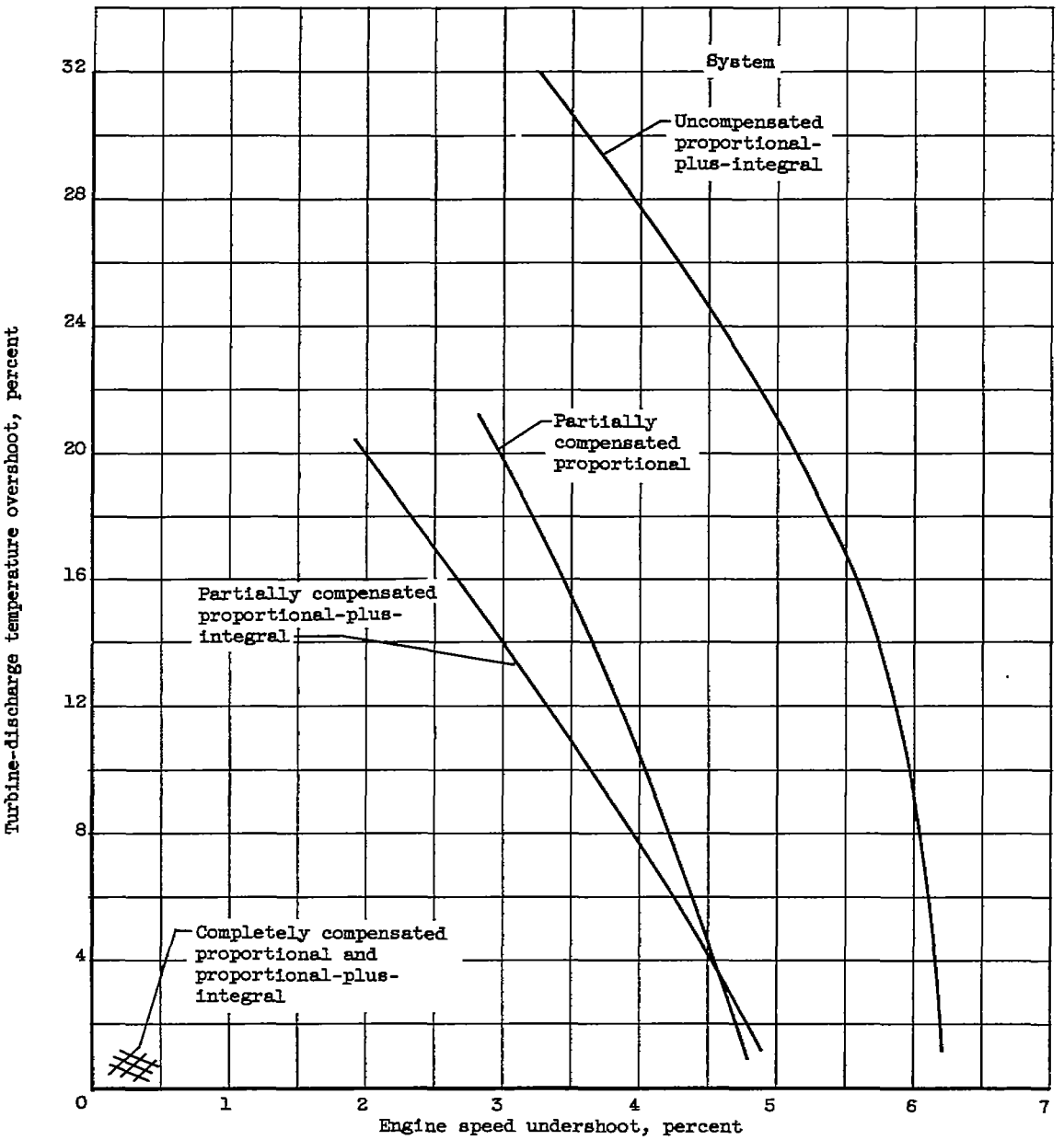

Figure 14. - Comparison of permissible performance criteria for five systems investigated; $\Delta A'_{eq,b} = -40\ U(t)$.